# Sugar beet pulp: Resurgence and trailblazing journey towards a circular bioeconomy

# Cellulosic Biomass-based Sustainable Hydrogels for Wastewater Remediation: Chemistry and Prospective

**Sourbh Thakur[a,b*], Ankit Verma[b], Vinod Kumar[c], Xiao Jin Yang[d], Satheesh Krishnamurthy[e], Frederic Coulon[c] and Vijay Kumar Thakur[f,g,h*]**

[a]*Department of Organic Chemistry, Bioorganic Chemistry and Biotechnology, Silesian University of Technology, B. Krzywoustego 4, 44-100 Gliwice, Poland*

[b]*School of Advanced Chemical Sciences, Shoolini University, Solan, 173229, Himachal Pradesh, India*

[c]*School of Water, Energy, and Environment, Cranfield University, Cranfield, United Kingdom*

[d]*Beijing Key Laboratory of Membrane Science and Technology, College of Chemical Engineering, Beijing University of Chemical Technology, 100029, Beijing, China*

[e]School of Engineering and Innovation, The Open University, Milton Keynes, MK7 6AA, United Kingdom

[f]*Biorefining and Advanced Materials Research Center, SRUC, Edinburgh EH9 3JG, UK*

[g]*Department of Mechanical Engineering, School of Engineering, Shiv Nadar University, Uttar Pradesh, 201314, India*

[h]School of Engineering, University of Petroleum & Energy Studies (UPES), Dehradun, Uttarakhand, India

***Corresponding authors Email**: Sourbh.Thakur@polsl.pl, thakursourbh@gmail.com, (Sourbh Thakur) Vijay.Thakur@sruc.ac.uk (Vijay Kumar Thakur)

**Abstract**

Despite several technological improvements and achievements, wastewater treatment remains a serious issue internationally. Toxins in wastewater pose a significant threat to human health if left untreated. Due to macro-porous structure and different surface functionalization, cellulose biomass-based hydrogel is the most traditional adsorbent for removing harmful ions from wastewater. Recently, the introduction of several new cellulose derived materials have demonstrated their competitiveness in the removal of harmful ions. Numerous exceptional qualities better define this promising material, including high mechanical strength, large surface area and chemical inertness. This paper discusses the development status, preparation and modification methods of cellulose composites created by various materials (graphene, fly ash, graphene oxide and bentonite) which evaluates the research development and existing challenges in water treatment.

**Keywords:** Cellulose; carboxymethyl cellulose; cellulose-based hydrogels; pollutants, wastewater remediation.

## 1. Introduction

Our society is comprehensively dependent on the use of plastics that are derived from petroleum feedstocks. Because of growing environmental concerns contiguous to plastic waste pollution and recycling problems, it is becoming ever imperative to look for nature-based resources wherever possible [1–4]. Pollution and climate change have emerged as two of the most conspicuous and significant problems that we will confront in our lifetime [5–7]. The scarcity of clean water supply in many developing nations may be owing to a failure to treat wastewater appropriately or to discharge effluent below an environmentally safe level to surrounding waterbodies [8,9]. Water

quality, in particular, has deteriorated in overpopulated countries such as India, Kenya, Ethiopia and Nigeria [10]. With high biological (BOD) and chemical oxygen demand (COD), wastewater contains significant volumes of organic and inorganic nutrients causing imbalance ecosystem [11]. Excess nutrients such as nitrogen (N) and phosphorus (P) can induce eutrophication of waterbodies [12].

With the current challenges, we are facing in terms of materials resources and pollution; there is an urgent need for more realistic ecological bio-based alternatives such as biopolymers; biocomposites, membrane and hydrogels. The cellulosic biomass derived from different natural resources offers a high potential to work as promising sustainable precursors for a cleaners and greener environment having advanced applications in water treatment, biomedical, soil remediation and pollution filtering to name a few using advanced synthesis and manufacturing techniques [13–16].

Hydrogels are one such kind of materials that can be used for both wastewater treatment and biomedical. The natural or synthetic molecular biomaterials which has a high degree of adsorption efficiency and who maintains a huge quantity of liquid in their turgid state known as hydrogels [1,17–20]. When placed in water or other biological fluids, hydrogel has ability to resist disintegration [21–25]. For example, polyethylene glycol can be cross-linked to form hydrogel having stereographic polymeric constructions that can suck up a huge amount of water which varies from few percent to hundreds of times in comparison to its dry weight [26–29]. The cross-linkage into various polymer chains is introduced with the help of a cross-linkage agent [30–33]. The cross-linkage between polymers takes place under two conditions: (a) *in vitro* i.e. during the time of formation of the hydrogel, (b*) in vivo* i.e. inside the human body after successful implementation on a specific site. The cross-linkage present among polymeric chains prevents its

66 decomposition in water and other fluids [31,34–36]. The vacant spaces among the three-
67 dimensional structure of the hydrogel are active sites for the uptake of water. This cross-linked
68 composition provides nature to the hydrogel which makes them good enough for use in biological
69 implants without any side effects [37–39]. The extent of expansion of hydrogels is measured based
70 on the number of cross-linked units and type of mixture having water-loving polymers or
71 copolymers. The tendency of the hydrogel to absorb maximum amount of liquid is hidden in its
72 amazing structure [40–43]. The polymeric structure contains hydrophilic moieties such as –
73 $CONH_2$, -COOH, $-NH_2$, -OH, $-SO_3H$ etc [44–46]. For example, Verma et al. (2020) prepared
74 sodium alginate-based hydrogels for elimination of malachite green dye and reported higher
75 adsorption tendency of 628.93 mg $g^{-1}$ [47]. The existence of rich quantities of –COOH groups in
76 the sodium alginate backbone, due to this prepared material showed strong interaction with
77 malachite green dye. In addition to traditional adsorption procedures, algae-based wastewater
78 treatment method is another tempting solution due to excellent fixation of inorganic substances
79 such as carbon dioxide and heavy metals [48]. Microalgae have high potential for inorganic
80 nutrient intake because they require nitrogen and phosphate for protein synthesis as well as heavy
81 metals as micronutrients for growth [10,49]. In this sense, the use of algae as wastewater
82 bioremediation agents can successfully take nitrogen and phosphorus out of wastewater, preserve
83 dissolved oxygen content and aid in the reduction of pathogens and faecal bacteria present in
84 wastewater [50].

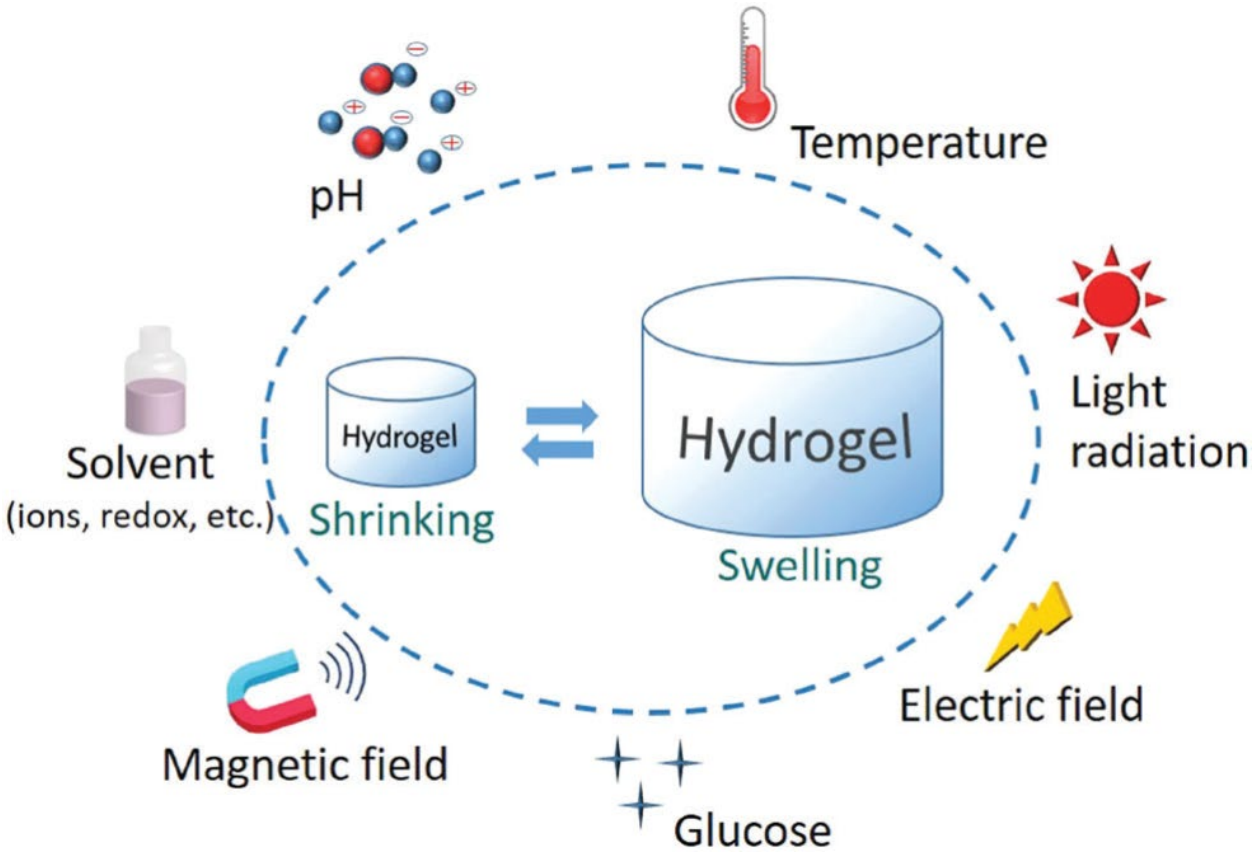


**Figure 1.** The schematic diagram for stimuli-responsive properties of hydrogels fabricated from cellulose [51].

The environmental stimuli like pH, light and solvent affected the swelling tendency of the hydrogels fabricated from cellulose **(Figure 1)**. The stimuli-responsive hydrogels fabricated from cellulose demonstrated the great potential in wastewater remediation. For example, in carboxymethyl cellulose, -$CH_2COOH$ groups present into its molecular chain plays a critical role in swelling and adsorption at different pH. The hydrophobic behaviour of carboxymethyl cellulose increases in an acidic medium because of the hydrogen bonding formed in its molecular chain. On the contrary, in basic medium, carboxyl groups present in the carboxymethyl cellulose chains can be ionized into carboxylate groups and increase the hydrophilic character of the carboxymethyl cellulose-based hydrogels. Pourjavadi et al. (2009) fabricated carboxymethyl cellulose-based

97 acrylamide and 2-acrylamido-2-methyl propane sulfonic acid hydrogel by free radical
98 polymerization and reported the maximum swelling (about 1400 g $g^{-1}$) at pH 7.
99 Cellulose is the most generous material which can be easily extracted from lignocellulosic
100 biomasses, in our literature survey, several pieces of research have prepared the pure cellulose
101 from natural cellulosic biomass waste. Worldwide production of cellulose is in between 75–100
102 billion tons, therefore could serve as an alternative material for petroleum/coal-based adsorbents.
103 Furthermore, cellulose-based hydrogels have promising properties that make them a first-rate
104 applicant for use in water-based remediation processes: (a) high specific surface area which
105 provides more active sites, (b) hydroxyl groups provides easy grafting of sulfate, ester, amine and
106 aldehyde functionalities has advantages in case of cellulose-based adsorbents across various water
107 remediation processes like membrane filtration, degradation, flocculation and absorption, (c) high
108 stability and surface tension of cellulose in water reduces the bio-fouling and enhances the wetting
109 characteristics and (d) colloidal stability and aggregation of cellulose affects the applicability and
110 efficacy of cellulose-based hydrogels in water remediation processes [52–54].
111 Based on origin, hydrogels are of two types natural and synthetic. Both types of hydrogels have
112 proved themselves in the field of adsorption. However, there are some problems associated with
113 synthetic hydrogels such as poor solubility and toxicity, toxic cross-linkers, unreacted monomer
114 units, highly crystalline composition [55]. These drawbacks stimulated the research to enhance the
115 properties and functionality of hydrogels [56–60]. Hence, hydrogels are of natural origin gradually
116 replacing manmade products. Natural hydrogels possess higher properties such as high flexibility,
117 high-temperature sustainability, biodegradable nature, non-toxic behaviour, easy incorporation in
118 the biological system and transport of pre-determined amount of drugs in a biological system
119 without any harmful effects [61–63]. In addition, natural hydrogels are of great synthetic utility

behaving as a superabsorbent with high mechanical strength, high elasticity and water holding capacity [64].

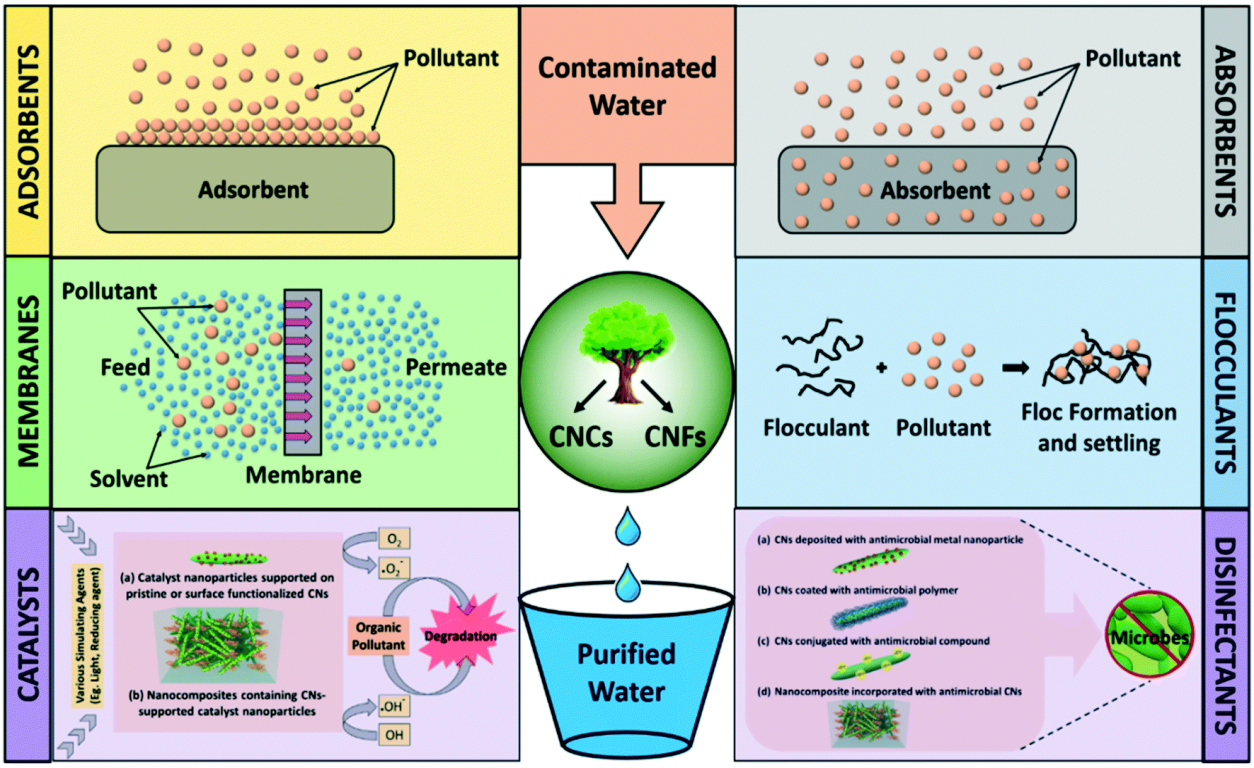


**Figure 2.** Different wastewater treatment techniques by using cellulose nanomaterials based systems [65].

For elimination of various toxins from contaminated water, variety of techniques have been employed, including precipitation, coagulation, reverse osmosis, adsorption, filtration with coagulation, ion exchange, ozonation and advanced oxidation processes [66–68]. Adsorption with the help of solid adsorbents from different biomass-based materials is an efficient technique for the remediation of toxins from contaminated water. Adsorption provides a number of advantages over other techniques, including a simple design and the potential for a minimal initial investment in terms of costs and land, it has drawn lot of interest from researchers [69]. The quest for low-cost adsorbents with pollutant-binding capabilities has escalated in recent years, low-cost adsorbents from locally accessible resources like natural materials, industrial wastes and

agricultural wastes are required for sustainable development [70,71]. There has been increasing research interest in the evolution of high-quality hydrogels, biocomposites and their application in the field of environmental remediation [72–74]. Several cellulose-based materials have been thoroughly explored for the alternate of expensive activated carbon and to prevent the use of additional costly and difficult remediation techniques like ion exchange, membrane filtration and chemical precipitation. Most of the published studies focus on reporting maximal adsorption capacities of cellulose-based materials under batch processes, the model pollutants are mostly synthetic in form, and the adsorption characteristics of the produced adsorbents have been investigated with just a few adsorbates in mind [75].

It is challenging to predict the prospective uses of these cellulose-based adsorbents in wastewater treatment and their removal effectiveness in real industrial effluents. Biodegradability, hydrophilicity, biocompatibility, chemical and thermal stability are the advantages of cellulose-based adsorbents [76]. Also, cellulose, which is ecologically beneficial and inexpensive, will replace petroleum-based materials [77]. Therefore, this review focused on cellulosic-based hydrogels applications for wastewater treatment applications (**Figure 2**).

## 2. Cellulose and carboxymethyl cellulose

The different sources of cellulose and applications of cellulosic hydrogels are summarized in **Figure 3a**. Cellulose is an extremely common biotic substance on Earth, with above one trillion tons of resources of cellulose present in nature. It is a renewable and ecological material that can give various valuable products after derivatization [78,81]. The major source of cellulose is ground flora. However, it is also present in fungi, algae, microbes and all land plants. The cellulosic content in cotton fibres is about 90 %, in bast fibres is 60-70 % and in wood is 45-50 % [82–84].

Cellulose is mainly the richest; they are produced in a sustainable technique and recommend many possibilities for use. It is an advantageous renewable, recyclable, biocompatible material that has a distinctive ability to generate a number of derivative products [85,86]. Despite such extensive properties, the major disadvantages are its luxurious manufacturing, its sensibility to water, and its sluggish regeneration [87,88]. Cellulose is a stereoregular, linear and semi-crystalline polysaccharide. Its macromolecules are oriented in a chair conformation containing D-glucopyranose (Anhydroglucose) units which are connected by head-to-tail 1,4-β glycosidic bonds. Additionally, cellulose does not exist as an individual molecule, almost 36 cellulose individual molecules are combined and form a large unit called elementary fibrils.

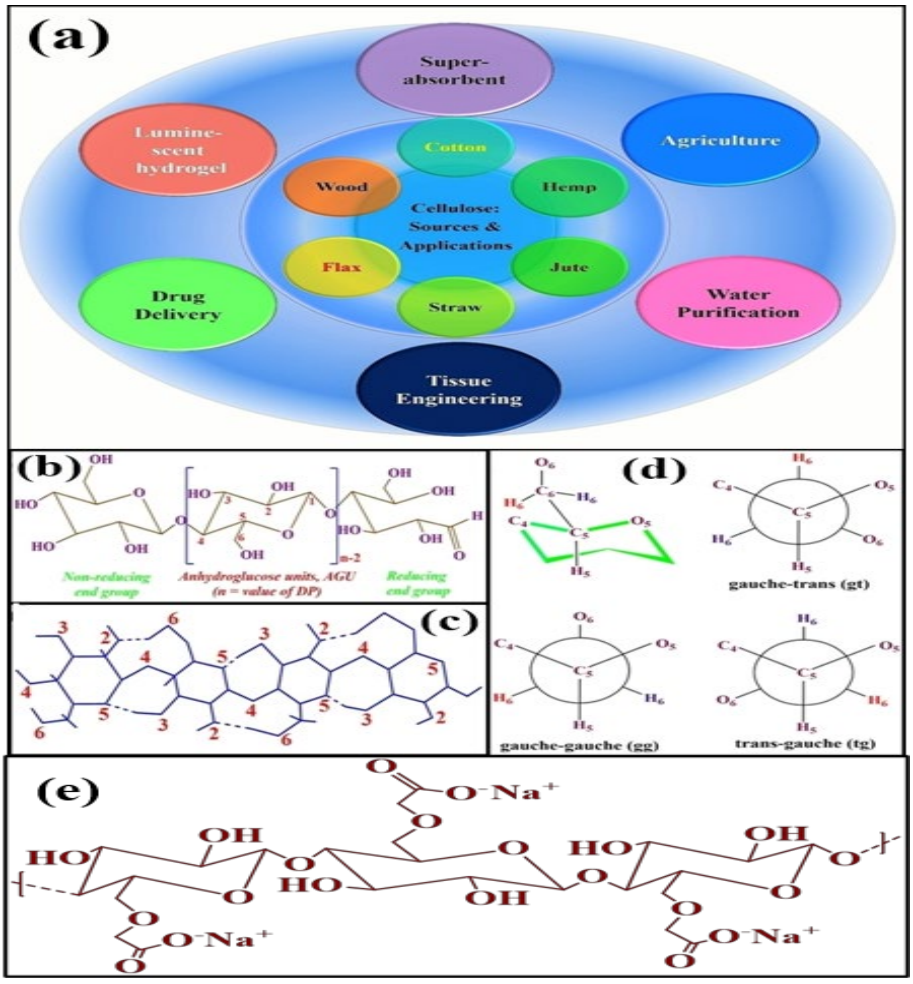

**Figure 3. (a)** Sources of the cellulose and different applications of hydrogels fabricated from cellulose, **(b)** cellulose construction and numbering of C-atom. Adopted from [78], **(c)** intermolecular hydrogen bonding between the cellulosic groups. Adopted from [79], **(d)** possible conformations: gauche–trans (gt), gauche–gauche (gg) and trans–gauche (tg). Adopted from [79] **(e)** molecular structure of sodium salt of carboxymethyl cellulose [80].

**Figure 3b** shows the anhydroglucose unit containing three reactive -OH groups on the C-2, C-3, and C-6 atoms which are generally available for the modification of secondary and primary -OH groups [79]. Hydrogen atoms are on the axial plane of the ring and anion OH groups are located on the equatorial plane. The chemical structure of cellulose is supported by an intermolecular hydrogen bond arrangement. This pre-established hydrogen bond extends from the O(3′)-H hydroxyl to the O(5) ring oxygen of the next unit transversely by the glycosidic linkage and from the O(2)-H hydroxyl to the O(6′) hydroxyl of the next residue is shown in the **Figure 3c**. In-chair conformation two different hydroxyl groups are present in which one hydroxyl group is on the $C_6$ carbon atom and the second is linked with ring carbon atom ($C_5$) **(Figure 3d)**. The primary anion OH introduces two different torsion angles, one is $O_5$-$C_5$-$C_6$-$O_6$ and the second is $C_4$-$C_5$-$C_6$-$O_6$. The $60^o$ and $180^o$ torsional angles are possessed by Gauche and Trans conformations respectively. The most possible three rotational conformations in the structure of cellulose are shown in **Figure 3d**.

Carboxymethyl cellulose is a cellulose derivative with excellent hydrophilic characteristics and great mechanical strength. Carboxymethyl cellulose is a naturally occurring anionic polysaccharide that is utilized in a variety of industries, such as textiles, food adhesives, paper, paints, cosmetics and medicines [89]. It is a non-toxic, reusable, abundantly accessible, biocompatible, and biodegradable natural polymer. It is amphiphilic because it contains a

hydrophobic polysaccharide backbone and several hydrophilic –COOH groups [90]. The molecular structure consists of the sodium salt of carboxymethyl cellulose as shown in **Figure 3e**. Mainly, cellulose is formed of glucose rings linked by –C(1)–O–C(4) ether bonds, commonly known as β -1,4 glycosidic linkages and contains a lot of intramolecular hydrogen [80]. Moreover, the characteristics of carboxymethyl cellulose are determined by the degree of hydroxyl group substitution, or through purity, crystallinity and molecular weight [91].

## 2.1. Production of cellulose-based hydrogel

Numerous strategies have been used for the preparation of hydrogels fabricated from cellulose [92]. It is feasible to develop various hydrogels based on cellulosic material as (a) hydrogels with the help of native cellulose, (b) hydrogels from cellulose derivatives and (c) hydrogels by mixing of cellulose or its derivatives with different polymers.

### 2.1.1. Cellulose native hydrogel

Hydrogel based on cellulose can be prepared with the help of cellulose solution through crosslinking. It can be effectively synthesized by hydrogen-bonded cross-linking because hydroxyl groups existed in the structure of cellulose. However, the widely expanded cellulose structure, which is hydrogen-bonded, as a result, structure is dense and difficult to dissolve in traditional solvents. Therefore, different solvents should be utilized to dissolve cellulose, newly developed solvents like ionic liquids, N-methylmorpholine-N-oxide and alkali/urea (or thiourea) aqueous solutions have been introduced with major applications in the field of hydrogels [93]. Moreover, the manufacturing of almost pure cellulose hydrogels requires some bacterial organisms [94]**.**

### 2.1.2. Cellulose derivatives hydrogel

The majority of cellulose derivatives are water-soluble and biocompatible. These can be utilized as thickeners, emulsifiers, binding agents, suspension supports, surfactants and particular in dairy, cosmetics and pharmaceutical companies. Derivatives of cellulose like hydroxypropyl cellulose, methylcellulose, hydroxypropyl methylcellulose and carboxymethyl cellulose can be utilized to produce hydrogel by chemical and physical crosslinking [95]. The physically crosslinked hydrogels are prepared by hydrogen bonding, ionic bonding or by the interaction between polymer-polymer chains. In this case, no creation or breakage of covalent bonding [92,96], chemically linked hydrogels is obtained by functionalized crosslinking of two or more polymeric networks [97].

### 2.1.3. Hydrogels from mixing of different polymers

A desirable, economical and beneficial approach for producing novel structural materials is the combining or merging of various polymers[98–100]. Novel structural materials for specific applications including biocomposites [101–103] have been developed using cellulose or its derivatives combined with other synthetic and natural polymers, like starch, lactic acid, chitosan, alginate and hyaluronic acid [92,104–106]. Cellulose-starch for the food industry [107], cellulose-chitosan for heavy metal removal [108] and cellulose-alginates for tissue engineering [109] are some examples of mixed cellulose polymer composite.

## 3. Cellulose-based hydrogels for wastewater remediation

A lot of technological research and development studies have been done on a variety of consolidated and emerging water purification technologies to provide compelling solutions to the water pollution problem [65,110–112]. Among others, the developments and the use of low-cost adsorbents for the removal of important aquatic contaminants such as activated carbon has gained

significant interest and while most of these adsorbents are claimed to have high efficiency > 99 %, this is often only valid under optimal conditions of pH, contaminant concentration and other operating parameters, which do not reflect environmentally genuine conditions [113–119]. Many of these adsorbents are also designed to target a limited number of contaminants at a time, which makes their use impractical for polluted waters. Cellulose-based hydrogels can help to overcome these issues and have been already utilized for organic dyes, heavy metals and other organic pollutants like pesticides, herbicides and organic compounds removal from aqueous solutions. **Table 1 and Table 2** summarize the outcomes from recent studies on hydrogels fabricated from cellulose for the removal of different types of toxins. It can be concluded from the tables that hydrogels fabricated from cellulose are effectively capable of the adsorption of all types of toxins such as dyes, metal ions, pesticides and other toxic organic molecules, but are more effective in removing dyes (lignin-holding hemicellulose-based hydrogel: 2691 mg $g^{-1}$ for methylene blue) in comparison with other toxic ions.

### 3.1. Cellulose-based hydrogels for organic pollutants

Organic polyphenol compounds, whether organochlorinated or aromatic, are recognised to be the most toxic to living beings and plants. The sources of such environmental contaminant materials are numerous from the pharmaceutical sector, leaching and drainage from agriculture and forestry land (by the usage of pesticides and weed killers) and hazardous waste disposal. In the absence of any procedure persistent organic contaminants, other chemicals, permanently collect inside water which promotes the possibility of pollution in underground sources [35,120]. Abdel Ghaffar et al., successfully prepared carboxymethyl hydrogels fabricated from cellulose through radiation grafting procedure, which is simpler, low cost, environmentally sustainable. The adsorption potential of poly(carboxymethyl cellulose/methacrylic acid) (1/20 wt%) hydrogel for both 4-

chlorophenol and 2,4 dichloro phenoxy acetic acid was found greater than that of poly(carboxymethyl cellulose/methacrylic acid: acrylamide) (1/60:40 wt%). It is attributed to the existence of more hydrogen bonding within the poly(carboxymethyl cellulose/ methacrylic acid: acrylamide) hydrogel which inhibits the adsorption of pollutants.

Gupta et al., synthesized the composite membrane through choline chloride blended cellulose acetate and coated on a fly-ash dependent ceramic substrate for successful elimination of phenol [121]. Choline chloride blend has important effects on membrane characteristics like swelling, pore depth, chemical stability, permeability, and hydrophilicity. In the analysis of phenol removal, the removal percentage was reduced with increased pressure and concentration of feed phenol, in contrast, improved with pH rise. Hence, 0.9 % of choline chloride blended cellulose acetate can be used to produce the necessary composite membrane for high phenol removal. Aouada et al., synthesized the methylcellulose and poly(acrylamide) hydrogel for extracting paraquat [122]. A free-radical polymerization process was used to prepare poly(acrylamide)/methylcellulose hydrogels with varying amounts of acrylamide and methylcellulose. The acrylamide, methylcellulose and paraquat concentrations significantly affected the adsorption ability of hydrogels and the highest adsorption tendency was 14.3 mg $g^{-1}$ with 6 % acrylamide and 0.75 % methylcellulose. In this adsorption process, Freundlich isotherm performed better than the Langmuir isotherm which means a heterogeneous surface. These findings indicate the poly(acrylamide)/ methylcellulose hydrogels are potentially possible absorbent for extracting paraquat herbicide.

275 **Table 1.** Cellulose-based hydrogels for removal of organic pollutants.

| Sr. No. | Hydrogels | Fillers | Starting materials | Organic Pollutants (dyes) | Optimized parameters | Maximum adsorption capacity | References |
|---|---|---|---|---|---|---|---|
| **1.** | Cellulose nanofibrils-graphene nanoplates aerogel | Carbon nanotubes, Graphene nanoplates | Cellulose, Sodium chlorite, potassium hydroxide, sodium hypochlorite, 2,2,6,6-tetramethylpyperdine-1-oxyl | Methylene blue<br>Congo red | Adsorbent dose = 0.005g,<br>Temperature = 25°C | 1178.5 mg $g^{-1}$<br>585.3 mg $g^{-1}$ | [123] |
| **2.** | Cellulose-based bio adsorbent | - | Hyperbranched polyethyleneimine, Glutaraldehyde, Cellulose powder | Reactive yellow, Bright yellow and Disperse brown | Adsorbent dose = 0.1g,<br>pH = 7 for reactive yellow, bright yellow,<br>pH = 3 for disperse brown | 970.87 mg $g^{-1}$<br>571.43 mg $g^{-1}$<br>581.40 mg $g^{-1}$ | [124] |
| **3.** | Carboxymethyl cellulose grafted poly (3-sulfopropylmethacrylate) hydrogel | - | Carboxymethyl cellulose sodium salt, 3-Sulfopropyl methacrylate potassium salt, N, N′-methylenebisacrylamide | Methylene blue | Adsorbent dose = 0.05g,<br>pH = 6,<br>Temperature = 25°C | 1675 mg $g^{-1}$ | [125] |
| **4.** | Carboxymethyl cellulose-acrylamide-graphene oxide hydrogel | Graphene oxide | Carboxymethyl cellulose, Acrylamide, Ammonium persulphate, N, N′-methylenebisacrylamide, Potassium permanganate, Natural | Acid Blue-133 | Adsorbent dose = 0.1g,<br>pH = 6,<br>Temperature = 20±2°C | 185.45 mg $g^{-1}$ | [126] |

| | | | | | | | |
|---|---|---|---|---|---|---|---|
| | | | graphite powder, Hydrogen peroxide, Sodium nitrate, Sulfuric acid | | | | |
| **5.** | Lignin-holding hemicellulose-based hydrogel | - | Acrylic acid, Ammonium persulphate, N, N, N', N'-tetramethyl-ethane-1, 2-diamine, sodium lignosulfonate | Methylene blue dye | Adsorbent dose = 0.05g, pH = 10, Temperature = 30°C | 2691 mg $g^{-1}$ | [127] |
| **6.** | Pineapple peel cellulose-based sepia ink hydrogel composite | Sepia ink | Ionic liquid 1-butyl-3-methylimidazolium chloride, Pineapple peel cellulose, sodium chlorite, potassium hydroxide, polyethylene glycol | Methylene blue dye | - | 138.25 mg $g^{-1}$ | [128] |
| **7.** | Cellulose/sodium alginate hydrogel composite | - | Cellulose, Sodium alginate, Sodium chloride, Calcium chloride | Methylene blue dye | Adsorbent dose = 0.445g, pH = 7, Temperature = 25°C | 256.41 mg $g^{-1}$ | [129] |
| **8.** | Waste cellulose-based glycidyl methacrylate composite | - | Cellulose waste, Glycidyl methacrylate, acetate and phosphate buffer solutions | Acid-fast yellow, acid methyl blue, acid methyl green | Adsorbent dose = 0.5g, pH = acidic, Temperature = 20°C | - | [130] |
| **9.** | Carboxymethyl cellulose-based poly (acrylic acid)/bentonite composite membrane | Bentonite | Carboxymethyl cellulose, potassium persulfate, glutaraldehyde, N, N' - methylene-bis-acrylamide, 1,5 diphenyl carbazide | Crystal violet | Adsorbent dose = 0.1g, Temperature = ~20°C | 546 mg $g^{-1}$ | [131] |

| Other organic pollutants (Pesticides, organic compounds) | | | | | | | |
|---|---|---|---|---|---|---|---|
| **1.** | Choline Chloride Blended Cellulose Acetate-Fly Ash Composite Membrane | Fly ash | Cellulose acetate, choline chloride, polyethylene glycol, fly ash, boric acid, sodium metasilicate, sodium carbonate | Phenol | Phenol concentration = 100 mg $L^{-1}$, pH = 10 | 92.7% | [121] |
| **2.** | Cellulose acetate–supported membrane, Imidazole-based ionic liquid | - | Cellulose acetate, 2-ethyl imidazole salt, 2-bromopropyl amine hydrobromide, toluene, ethyl acetate | Pirimicarb | Adsorbent dose = 0.01g, Temperature = 50°C | 74%, 68% | [132] |
| **3.** | Carboxymethyl cellulose based methacrylic acid hydrogel, Carboxymethyl cellulose methacrylic acid/acrylamide hydrogel | - | Carboxymethyl cellulose, acrylamide, methacrylic acid, | 4-chlorophenol, 2,4-dichlorophenoxyacetic acid | - | - | [120] |
| **4.** | Methylcellulose based poly(acrylamide) hydrogel | - | Methylcellulose poly(acrylamide), N, N' -methylene-bis-acrylamide, Sodium persulfate, N, N, N', N'-tetramethyl ethylene-diamine | Paraquat dichloride | - | 14.3 mg $g^{-1}$ | [122] |

276

277

278 **Table 2.** Cellulose based hydrogels for removal of inorganic pollutants.

| Sr. No. | Hydrogel | Fillers | Starting materials | Inorganic pollutants | Optimized parameters | Maximum adsorption capacity | References |
|---|---|---|---|---|---|---|---|
| **1.** | Cellulose based adsorbent | - | Quaternized cellulose, Polyethylenimine, 3 -chloro - 2 - hydroxypropyl trimethylammonium chloride, Epichlorohydrin, | Cr(VI) | Adsorbent dose = 0.05g, pH = 2, Temperature = 30°C | 490.3 mg $g^{-1}$ | [133] |
| **2.** | Fe(III)-complexed carboxylated cellulose beads adsorbents | Fe(III) | 2,2,6,6- Tetramethylpiperidine-1-oxyl, sodium hypochlorite, Sodium hydroxide, sodium chloride, $FeCl_3$ | $Br^-$ | Adsorbent dose = 5g, pH = 7, | 1.22 mg $g^{-1}$ | [134] |
| **3.** | Multiple active sites cellulose-based adsorbent | - | Microcrystalline cellulose, Epichlorohydrin, tetraethylenepentamine, bis(carboxymethyl) trithiocarbonate | Cu(II)<br>Pb(II)<br>Cr(VI) | - | 100 %<br>98 %<br>99 % | [135] |
| **4.** | Carboxymethyl cellulose and chitosan derived nanostructured sorbents | - | Sodium carboxyl methylcellulose, Chitosan, polyethyleneimine, tris(hydroxymethyl) -aminomethane | Cd(II)<br>Cr(VI) | Adsorbent dose = 0.02g, pH = 5 for Cd(II), pH = 2 for Cr(VI) | 470.0 mg $g^{-1}$<br>347.0 mg $g^{-1}$ | [136] |
| **5.** | Wheat straw cellulose-g-poly (acrylic acid)/poly (vinyl alcohol) hydrogel | | Sodium sulfite, acrylic acid, potassium persulfate, poly (vinyl alcohol), ammonium cerium nitrate, N,N'-methylenebisacrylamide | Cu(II) | - | 142.7 mg $g^{-1}$ | [137] |
| **6.** | Maleic anhydride modified | - | Diatomite, hydroxylamine hydrochloride, dithizone, $CaCO_3$ | Pb(II) | Adsorbent dose = 0.01g per 10 mL (10mg $L^{-1}$ | 44 mg $g^{-1}$ | [138] |

| | | | | | | | |
|---|---|---|---|---|---|---|---|
| | cellulose/diatomite beads | | powder, maleic anhydride, urea, acetone | | Pb concentration), pH = 6, Temperature = 30°C | | |
| **7.** | Sugarcane cellulose-based bio-adsorbent | | Sugarcane bagasse cellulose fiber, Epichlorohydrin, ethylenediamine, carbon disulfide, carboxymethylcellulose sodium | Cu(II) Zn(II) Pb(II) | - | 446.2 mg $g^{-1}$ 363.3 mg $g^{-1}$ 558.9 mg $g^{-1}$ | [139] |
| **8.** | Cellulose based poly-ethylene imine composite | - | Cellulose, poly (ethylene imine), epichlorohydrin, urea, lithium hydroxide | Cu (II) | Adsorbent dose = 0.01g, pH = 5, Temperature = room temperature | 285.7 mg $g^{-1}$ | [140] |
| **9.** | Carboxymethyl cellulose based poly (acrylic acid)/bentonite composite membrane | Bentonite | Carboxymethyl cellulose, potassium persulfate, glutaraldehyde, N,N' -methylene-bis-acrylamide, 1,5 diphenylcarbazide | Cd (II) | - | 781mg $g^{-1}$ | [131] |
| **10.** | Cellulose based collagen hydrogel beads | - | Microcrystalline cellulose, collagen powder, 1-butyl, 3-methylimidazolium chloride, $Na_2SO_4$ | Cu(II) | Adsorbent dose = 0.05g, pH = 6, Temperature = 19.85°C | 1.06 $mmolg^{-1}$ | [141] |
| **11.** | Cellulose based polyacrylamide/ hydroxyapatite hydrogel composite | Hydroxya patite | microcrystalline cellulose, N, N-dimethylformamide, Acrylamide, N,N' -methylenebis (acrylamide), potassium persulphate | Cu(II) | Adsorbent dose = 0.04g, pH = 5.8, Temperature = 20±1°C | 175 mg $g^{-1}$ | [142] |

| | | | | | | | |
|---|---|---|---|---|---|---|---|
| **12.** | Cellulose-based acrylamide hydrogel | - | Depithed bagasse, sulfuric acid, sodium hypochlorite, Acrylamide, potassium persulfate, glutaraldehyde | Cu(II)<br>Cr(VI) | - | 90.12%<br>94.2% | [143] |
| **13.** | Carboxy methylated cellulose-based chitosan physical hydrogel | - | Carboxymethylated cellulose, chitosan, acetic acid, | Cu (II)<br>Cd(II)<br>Zn(II) | Adsorbent dose = 0.2g,<br>pH = 5 for Cu(II),<br>pH = 6 for Cd(II)<br>pH = 5.5 for Zn(II) | 53.2 mg $g^{-1}$ (Cu (II)) | [144] |

279

### 3.2. Cellulose-based hydrogel for organic dyes adsorption

Mittal et al., prepared the carboxymethyl cellulose and chitosan crosslinked graphene oxide hydrogel nanocomposite for removal of organic dyes [145], highest removal tendency were 404.5 mg $g^{-1}$ for methyl orange (anionic dye) and 655.9 mg $g^{-1}$ for methylene blue (cationic dye) calculated from Langmuir isotherm model, regeneration tendency was reported for twenty adsorption-desorption cycles. Yu et al. (2020) developed hybrid aerogels using cellulose nanofibrils (CNFs), carbon nanotubes (CNTs) and graphene nanoplates (GnPs). The prepared aerogel was utilized for adsorption of methylene blue (cationic dye) and congo red (anionic dye) dyes. The prepared aerogels showed maximal adsorption capacities of 1178.5 mg $g^{-1}$ (cationic dye) and 585.3 mg $g^{-1}$ (anionic dye). The SEM images of prepared aerogels and adsorption mechanism for congo red and methylene dye is presented in **Figure 4**.

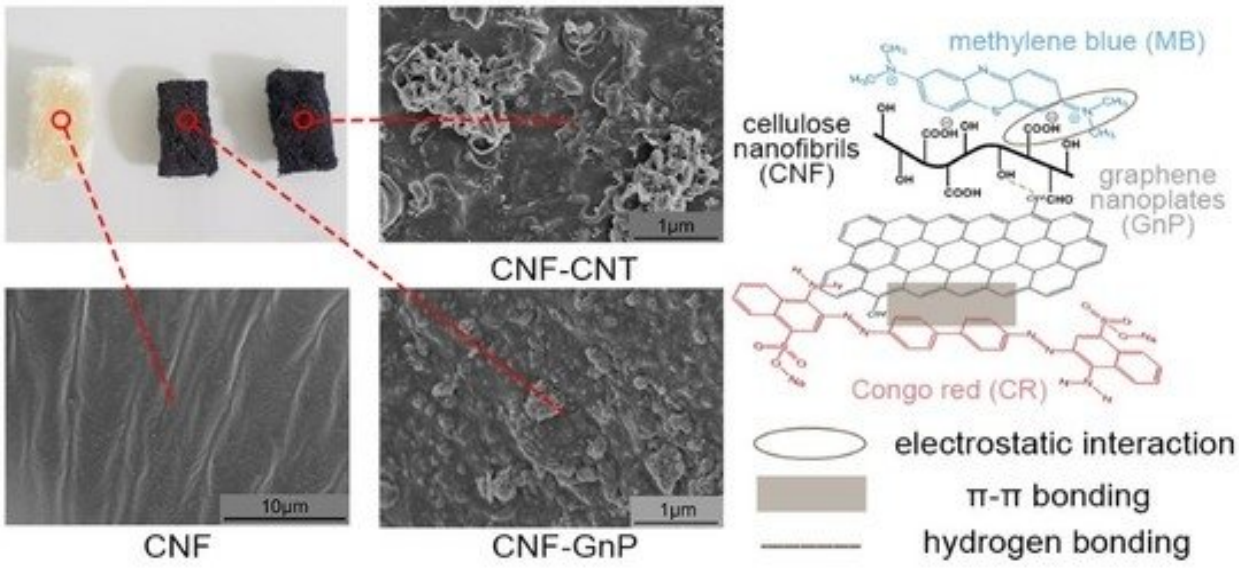


**Figure 4.** SEM images of hybrid aerogels and a possible mechanisms for the adsorption of congo red and methylene blue dyes [123].

The SEM analysis proved the fact that aerogels have large air pockets well suited for more adsorption rates. Prepared cellulose nanofibrils have shown irregular shapes of pores which were due to the high suspension concentration before the freeze-drying. Whereas, carbon nanotubes and graphene nanoplates showed the stacked aggregation between the particles which was probably because of strong binding between the individual particles. In comparison with the individual CNTs or GnPs, hybrid structures have shown a more porous network that facilitates a fast diffusion rate of molecules with enhanced accessible adsorption sites to the selected dye molecules. The aerogel demonstrated the best adsorption towards the contaminants when the CNTs and GnP ratio was 3:1. The hybrid ratio was another important parameter to analyse the best adsorption rate for the prepared adsorbent. Hybrid structures are mechanically strong and possess more adsorption sites than individual structures, which means tailoring cellulose to some hybrid structures advances the rate of adsorption more efficiently.

In another study, Chen et al., (2018) synthesized a cellulose loaded adsorbent by using modified hyper-branched polyethyleneimine with the help of glutaraldehyde [146]. The prepared sample was used for the elimination of anionic, cationic and non-ionic dyes. The reported adsorption capacity for reactive yellow X-RG (anionic), bright yellow M-7G (cationic) and disperse brown S-3RL (non-ionic) were 970.87 mg $g^{-1}$, 571.43 mg $g^{-1}$ and 581.40 mg $g^{-1}$, respectively. Comparative FTIR spectrum of pure cellulose and prepared bio-adsorbent are represented in **Figure 5a**. The peaks at 1430 $cm^{-1}$, 1579 $cm^{-1}$ and 1656 $cm^{-1}$ in the bio-adsorbent spectra were due to C-N stretching vibration, C=N stretching vibration and N-H bending vibration, respectively. The peaks at 3349 $cm^{-1}$ in pure cellulose were transferred to 3402 $cm^{-1}$ in the prepared bio-adsorbent spectra because of overlapping of O-H and N-H stretching vibration [147]. These results revealed the fact that the aldehyde group of glutaraldehyde undergoes a chemical reaction with an

amino group of polyethyleneimine which confirms the presence of a Schiff base structure. The peaks at 2923 and 2848 $cm^{-1}$ were attributed to $–CH_2$ stretching vibration, at 771 $cm^{-1}$ was attributed to C-H bending vibration and also explained the successful introduction of hyper-branched polyethyleneimine in the cellulose. The XPS spectra of pure cellulose and prepared bio-adsorbent are represented in **Figure 5b.**

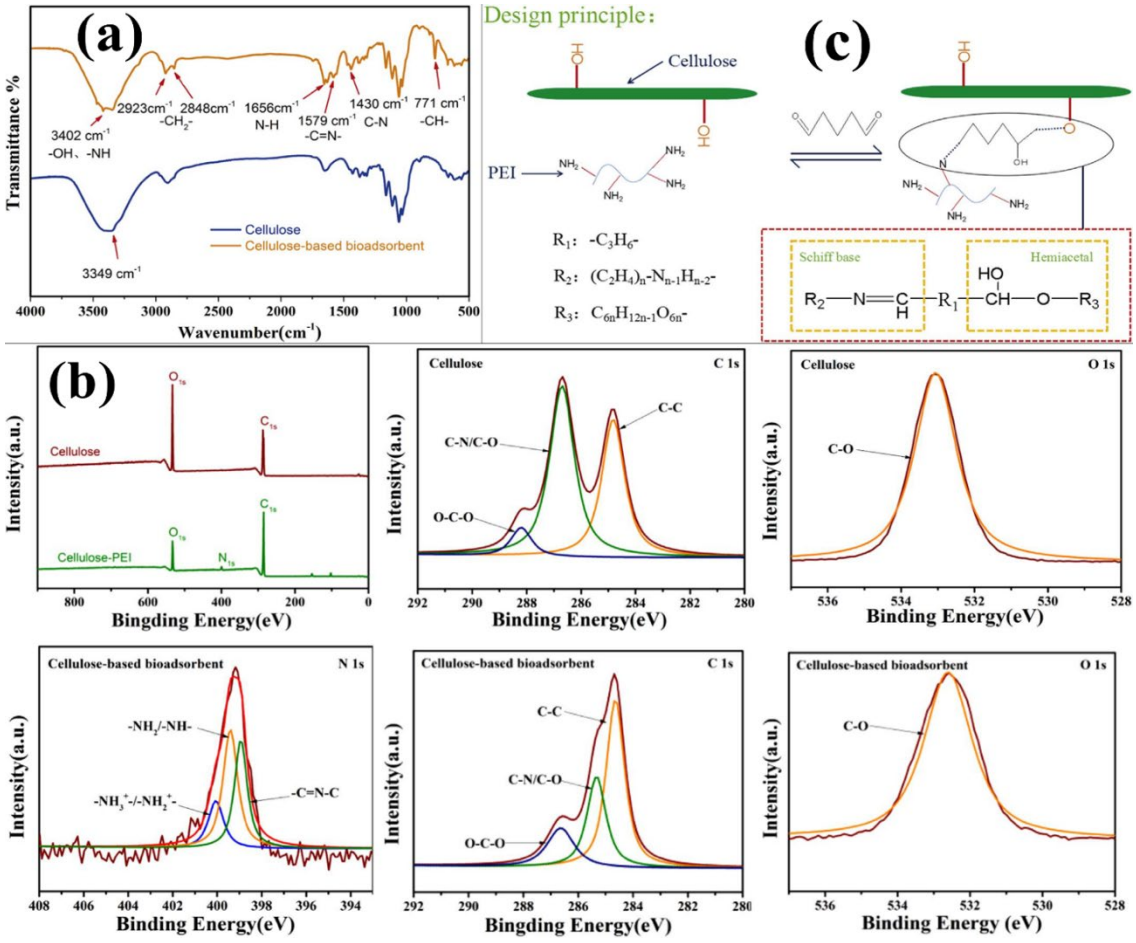


**Figure 5. (a)** FTIR spectra of pure cellulose and prepared bio-adsorbent [124]. Reprinted with permission from [124]. Copyright 2018 Elsevier, **(b)** XPS spectrum of pure cellulose and prepared bio-adsorbent [124]. Reprinted with permission from [124]. Copyright 2018 Elsevier, **(c)** proposed mechanism for the synthesis of bio-adsorbent [124]. Reprinted with permission from [124]. Copyright 2018 Elsevier.

328 The same elements C 1s and O 1s were present in pure cellulose and prepared bio-adsorbent but
329 one new element N 1s was introduced in the prepared bio-adsorbent showed modification by
330 hyper-branched polyethyleneimine. The three peaks of C 1s at 288.2 eV, 286.7 eV and 284.8 eV
331 were attributed to O-C-O, C-O/C-N and C-C respectively. After the modification by hyper-
332 branched polyethyleneimine, three peaks of C 1s were shifted to 286.6 eV, 285.3 eV and 284.6 eV
333 or the intensity of the peaks decreased. The peak of O 1s at 533 eV was corresponded to C-O/C-
334 OH [148] but shifted to 532.6 eV after the modification with hyper-branched polyethyleneimine.
335 The peaks of N 1s at 398.8 eV and 399.4 eV were due to C=N-C and $–NH_2$/-NH- respectively
336 confirmed the grafting of hyper-branched polyethyleneimine on the cellulose. FTIR and XPS
337 results supported the grafting of hyper-branched polyethyleneimine on the pure cellulose chain.
338 The possible mechanism for the preparation of bio-adsorbent is represented in **Figure 5c.** The
339 proposed mechanism showed the functional modification on cellulose with the help of hyper-
340 branched polyethyleneimine and glutaraldehyde.

341 Song et al., (2016) prepared lignin-supported hemicellulose hydrogel using acylated hemicellulose
342 (AHC), acrylic acid, N, N, N', N'-tetramethylethane-1,2-diamine, ammonium persulfate and
343 sodium lignosulfonate (NaLS) through free radical polymerization technique. The prepared
344 hydrogel was utilized for the elimination of methylene blue (MB) dye and the reported adsorption
345 tendency was 2691 mg $g^{-1}$. After four successive cycles, the adsorption capacity for MB dye was
346 about 80%. The nuclear magnetic resonance spectra of the pure hemicellulose (HC) and acylated
347 hemicellulose (AHC) showed the signals at 5.8, 6.6 ppm and 3.0 to 4.5 ppm which confirmed the
348 presence of protons for -CH=CH- group and pyran ring of xylan, respectively [149]. Also, the peak
349 at 4.4 ppm represented the anomeric proton of the pyran ring of xylan. The FTIR spectra of
350 hemicellulose, sodium lignosulfonate, acylated hemicellulose and Gel-3 (0.3 gm of acylated

hemicellulose and 0.1 gm of sodium lignosulfonate) was discussed. The broad bands at 1728 and 1638 $cm^{-1}$ were because of carbonyl group and C=C double bond of the acylated hemicellulose respectively [150]. Additionally, the bands at 1515 and 1124 $cm^{-1}$ were emanated from the aromatic ring and sulfonate group, respectively. These bands clearly showed the existence of sodium lignosulfonate in the Gel-3. Morphology of the synthesized lignin-based hemicellulose hydrogel with different sodium lignosulfonate dosages was presented. The porosity of lignin-based prepared hydrogel was changed significantly with the different amounts of sodium lignosulfonate. SEM monograph of the hydrogel free from sodium lignosulfonate (NaLS) named Gel-1. Gel-3 type of hydrogel containing 0.1 gm of lignosulfonate showed greater porosity than Gel-1. Gel-3 had reported the maximum adsorption capacity and swelling ability. The prepared lignin supported cellulose is not well suited for the cyclic economic ability concept as it lost efficiency at fourth cycle (80 %), whereas some researchers have reported recyclability of their material who maintains efficiency up to or above 90 % even after five adsorption-desorption cycles. In another work, Salama (2018) prepared superabsorbent hydrogel by grafting poly (3-sulfopropyl methacrylate) onto carboxymethyl cellulose. The prepared superabsorbent hydrogel was utilised for the adsorption of methylene dye at optimized pH 6. The higher reported adsorption efficiency of the superabsorbent was 1675 mg $g^{-1}$. After five cycles, the adsorption percentage of superabsorbent hydrogel was 89%. The possible mechanism for the interaction of methylene blue and prepared superabsorbent is shown in **Figure 6A**. The hydrogel composites based on the cellulose of pineapple peel and sepia ink from cuttlefish were prepared through homogeneous acetylation of cellulose [128]. In this technique, acetylation of cellulose was performed in the presence of ionic 1-butyl-3-methylimidadazolium chloride (BmimCl) liquid. The prepared adsorbent material was used for elimination of methylene blue. The removal efficiency was sharply increased from 53.72

to 138.25 mg $g^{-1}$ after adding the different concentrations of sepia link. Comparative FTIR spectrums of prepared samples are shown in **Figure 6B**. Peaks of sepia ink at 1368 $cm^{-1}$, 3224 $cm^{-1}$, 1578 $cm^{-1}$ were assigned to C-N stretching of amino acids, -OH and –NH stretching vibrations, ionized COO- and C=O double bond respectively [151]. FTIR of pineapple peel cellulose showed a broad peak at 3400 $cm^{-1}$ corresponded to the -OH group and a small peek at 2900 $cm^{-1}$ resulted from C-H stretching vibration. Similarly, FTIR of PPCAS-$M_6$ (sepia ink/BmimCl by wt.= 10%) and PPCA (sepia ink/BmimCl by wt.= 0%) hydrogel confirmed the acetylation via corresponding peaks at 1723 $cm^{-1}$ and 1168 $cm^{-1}$ because of C=O and C-O stretching's respectively. Additionally, none of the peaks at 1723 $cm^{-1}$ and 1168 $cm^{-1}$ were reported for PPCS (without acetylation of pineapple peel cellulose) hydrogel which means monoester of cellulose was produced in BmimCl liquid via acetylation.

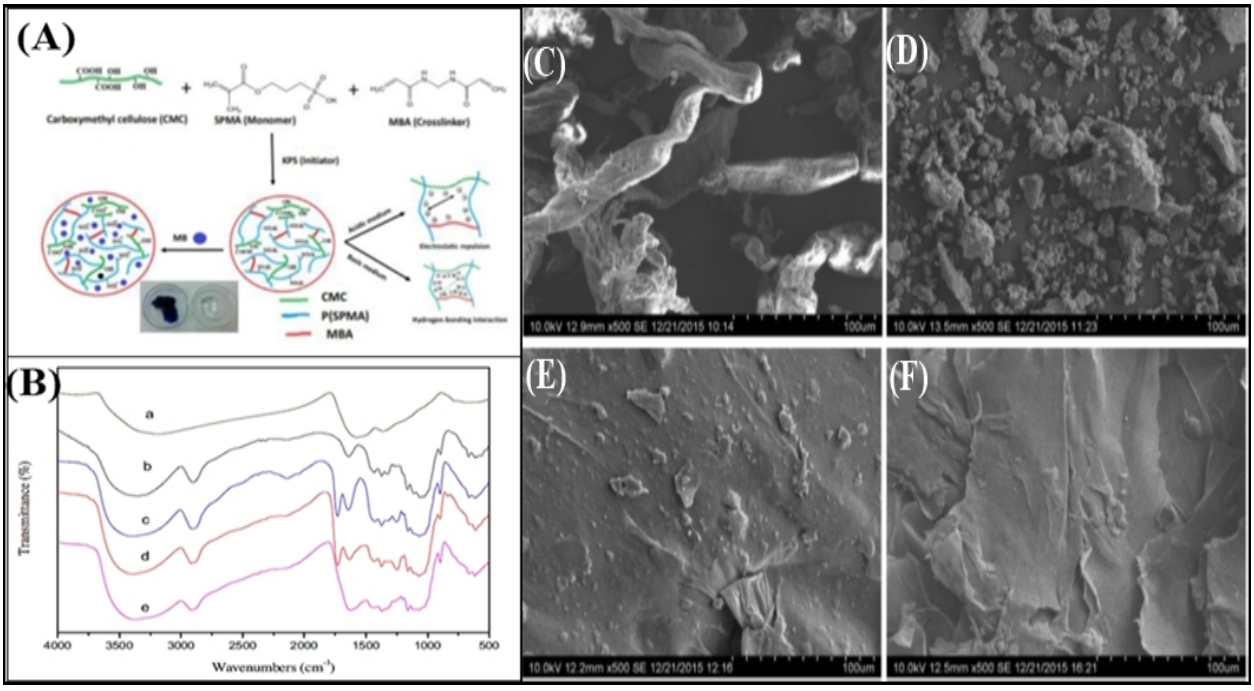


**Figure 6. (A)** Schematic representation for synthesis of superabsorbent hydrogel by grafting of poly (3-sulfopropyl methacrylate) onto carboxymethyl cellulose [125]. Reprinted with permission

from [125]. Copyright 2018 Elsevier, **(B)** FTIR spectra of (a) sepia ink, (b) pineapple peel cellulose, (c) PPCAS-$M_6$ hydrogel (sepia ink/BmimCl by wt.= 10%), (d) PPCA hydrogel (sepia ink/BmimCl by wt.= 0%) and (e) PPCS hydrogel (without acetylation of pineapple peel cellulose) [128]. Reprinted with permission from [128]. Copyright 2016 Elsevier, FESEM images of **(C)** pineapple peel cellulose, **(D)** sepia ink, **(E)** PPCAS-$M_6$ hydrogel (sepia ink/BmimCl by wt.= 10%) and **(F)** PPCA hydrogel (sepia ink/BmimCl by wt.= 0%) [128]. Reprinted with permission from [128]. Copyright 2016 Elsevier.

Furthermore, **Figure 6** shows the FESEM monographs of the prepared hydrogel composites. The fibre-like rough surface was observed in pineapple peel cellulose **(Figure 6C)**. The image of sepia ink showed small granules having a diameter of 200 μm to 100 μm **(Figure 6D)**. In comparison with the pineapple peel cellulose, PPCAS-$M_6$ (sepia ink/BmimCl by wt.= 10%) hydrogel and PPCA (sepia ink/BmimCl by wt.= 0%) hydrogel showed the noticeable change from granular to a smooth surface **(Figure 6E, F)** [152]. However, the disappearance of granular structures from the surface of PPCAS-$M_6$ confirmed the successful grafting of sepia ink onto the hydrogel matrix. Hence, sulfonate groups can enhance the adsorption rate of cellulose-based hydrogels. Researchers can apply the sulfopropyl methacrylate potassium salt as an ion-exchanger for an effective wastewater remediation.

Cellulose/sodium alginate hydrogel was fabricated by Mohammed et al., in 2015. Cellulose nano-particles were acquired from pulp fibres [129]. The synthesized hydrogel was utilized for adsorption of methylene blue dye. The reported adsorption tendency of hydrogel was 256.41 mg $g^{-1}$. The prepared sample had shown a good absorption tendency (~97 %) after five reuse cycles. Morphology and porosity of the sodium alginate and cellulose/sodium alginate hydrogel were examined by scanning electron microscopy (**Figure 7**). The less-dense and plane surface of pure

sodium alginate was observed **(Figure 7a)** but the density and roughness of the surface sharply increased on the addition of cellulose nanocrystal [153] **(Figure 7b)**. Additionally, cross-linking and porous behaviour of cellulose/sodium alginate hydrogel were noted (**Figure 7c,d)**. The reusability of the cellulose/sodium alginate hydrogel is represented in **Figure 7e**. In conclusion, it is a new generation recyclable approach that reduces our dependence on activated carbon because this material is cheap, reusable and mechanically strong. The modification of cellulose with alginate showed improved adsorption capacity than pure alginate hydrogels. Moreover, the adsorption efficiency of prepared hydrogel remained at ~ 97 %, after the five-time regeneration processes which is well described as cyclic economic material which can open its services on large industrial scale [154].

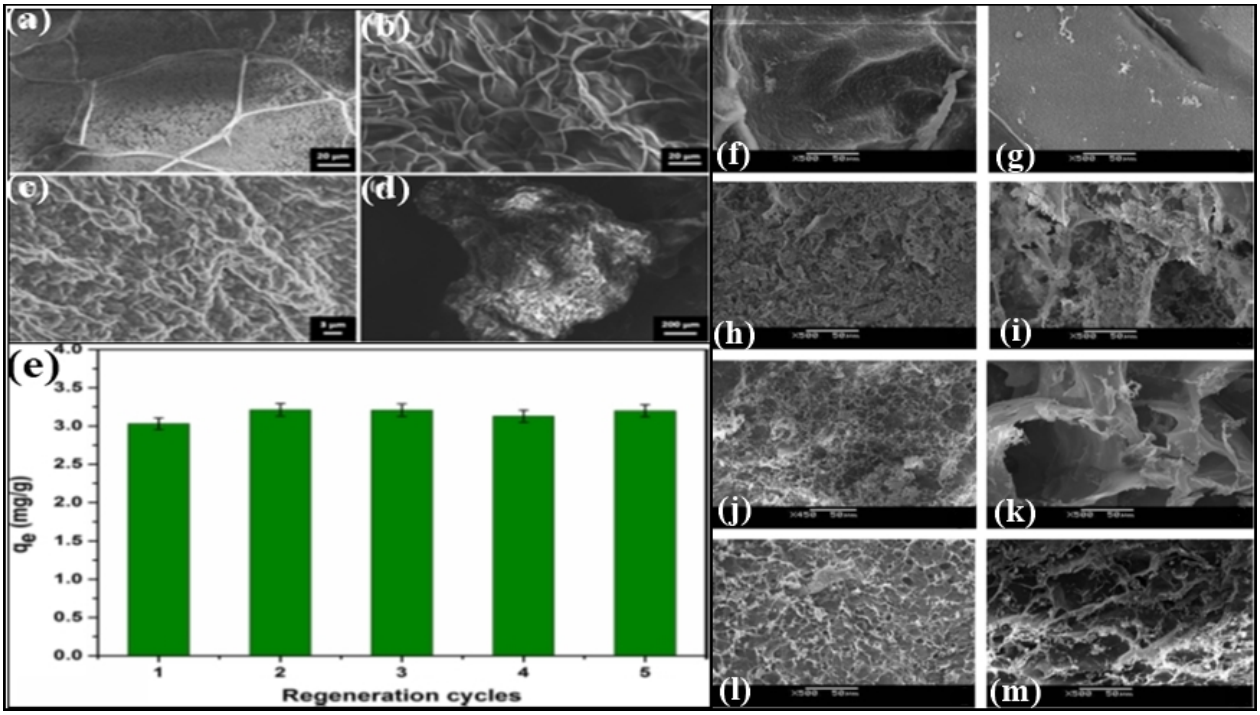


**Figure 7.** SEM images of **(a)** sodium alginate, **(b)** cellulose/sodium alginate hydrogel, **(c)** crosslinking behaviour of cellulose/sodium alginate hydrogel and **(d)** porous behaviour of cellulose/sodium alginate hydrogen [129]. Reprinted with permission from [129]. Copyright 2015

Springer, **(e)** reusability of the cellulose/sodium alginate hydrogel [129]. Reprinted with permission from [129]. Copyright 2015 Springer, SEM images of **(f, g)** pure cellulose hydrogel beads, **(h, i)** cellulose based collagen hydrogel beads (cellulose & collagen is 1:1), **(j, k)** prepared hydrogel (cellulose & collagen is 1:2), **(l, m)** prepared hydrogel (cellulose & collagen is 1:3) [141]. Reprinted with permission from [141]. Copyright 2013 Elsevier.

El-Kelesh et al. synthesized the waste cellulose-based glycidyl methacrylate composite [130]. In this study, firstly waste cellulose was treated chemically and then its grafting was done by using glycidyl methacrylate with the help of gamma rays and methanol/$H_2O$. The prepared composite was utilized for the adsorption of acidic dyes (acid-fast yellow, acid methyl blue, acid methyl green) from an aqueous solution. The reported maximum heat of adsorption values for acid-fast yellow, acid methyl blue and acid methyl green were 27.65, 34.77 and 38.81 KJ $mol^{-1}$ respectively. The IR spectroscopic analysis of pure cell (cellulose waste) and cell/glycidyl methacrylate-g-composite showed bands at 1187 $cm^{-1}$ and 2983 $cm^{-1}$ because of the stretching of C-O and C-H bonds respectively. Moreover, the band at 3223 $cm^{-1}$ was observed due to the O-H stretching of cellulose. The presence of intramolecular hydrogen bonding in cellulose was confirmed after the appearance of the band at 3495 $cm^{-1}$. Grafting of the cell via gamma radiations was confirmed by the appearance and disappearance of some peaks. A broad and intense peak in between the 3570-3050 $cm^{-1}$ range explained the formation of hydrogen bonds between non-substituted -OH groups and amino groups. With the help of scanning electron microscopy, the monographs of cellulose waste and cell/glycidyl methacrylate-g-composite were analysed. The pure cell was consisting of elementary fibres which were helical in shape and had less cellulosic polysaccharides whereas, in cell/glycidyl methacrylate-g-composite middle lamella was observed, which was present due to the grafting of thin layers of elementary cellulosic fibres. The thermal analysis for cellular waste

and cell/glycidyl methacrylate-g-composite was investigated under a nitrogen atmosphere. The three-step decomposition of pure cell and cell/glycidyl methacrylate-g-composite was observed. Weight loss of about 20 % for cell/glycidyl methacrylate-g-composite and about 8 % for the pure cell was observed in the first step of decomposition under the range of 50-230 ºC temperature and this was because of loss of water and $CO_2$ in the initial stage. In the second stage of decomposition, about 57% of weight loss was noticed within the range of 230-350 ºC which was because of the thermal degradation of cross-linked cellulosic chains. However, in the last step weight loss got increased within the increase in temperature from 400ºC to 450ºC for both cellulosic waste and glycidyl methacrylate -g-composite. From here it was concluded that pure cellulose showed higher mass loss than the prepared grafted composite material. Hence grafting enhanced the thermal stability of the polysaccharide structures. To sum up, researchers have introduced the radiation-induced grafting method, where no additive is needed for initiation. Importantly, cellulose is extracted from agricultural waste, which makes this approach non-toxic, biodegradable, biocompatible and easier to available. Another best part of their research is the optimization of the sample which is a key to get superior and steadier product quality.

### 3.3. Cellulose-based hydrogel for heavy metal ions adsorption

Godiya et al., fabricated the carboxymethyl cellulose based polyacrylamide hydrogel composite for Cu(II) Cd(II) and Pb(II) ions removal from aqueous solution [155], maximum adsorption efficiency were 227.2 mg $g^{-1}$ (Cu(II)), 256.4 mg $g^{-1}$ (Cd(II)) and 312.5 mg $g^{-1}$ (Pb(II)), adsorption experimental data followed the pseudo-second-order kinetics and Langmuir isotherm model. Singh et al., synthesized the cellulose-based aluminum oxide/ graphene oxide hydrogel for removal of fluoride ion from waste water [156], aluminum oxide nanoparticle was fabricated via a green method utilizing wastes generated during oil extraction from Syzygium aromaticum

(clove) and graphene oxide was chemically fabricated using pencil lead, reported adsorption tendency was 5.34 mg $g^{-1}$ in 2 hours at pH 5, experimental data best fitted for Langmuir isotherm model with 0.95 correlation coefficient value and pseudo second order kinetics model with 0.99 correlation coefficient value.

Wang et al. prepared the biodegradable cellulose-based collagen hydrogel beads, in 2013. The hydrogel beads were synthesized through reconstitution from 1-butyl, 3-methylimidazolium chloride solution [141]. There was a notable comparison between the removal efficiency of cellulose-based collagen hydrogel beads and cellulose-based hydrogel beads for Cu (II) ions. **Figure 7** shows the surface and cross-section morphology of pure cellulose hydrogel beads and cellulose-based collagen hydrogel beads (mass ratio of cellulose & collagen: 1:1, 1:2 and 1:3). The surface and cross-section of the pure cellulose hydrogel beads showed a dense and smooth surface **(Figure 7f,g)**. Then, adding the collagen microparticles to the hydrogel led to the porous and rigid surface (**Figure 7h,i)** and the porosity was continuously increasing with the increase in the number of collagen microparticles (**Figure 7j-m)**. Thus, the SEM images clearly explained the mass ratio of collagen microparticles affecting the porosity of the prepared cellulose hydrogel.

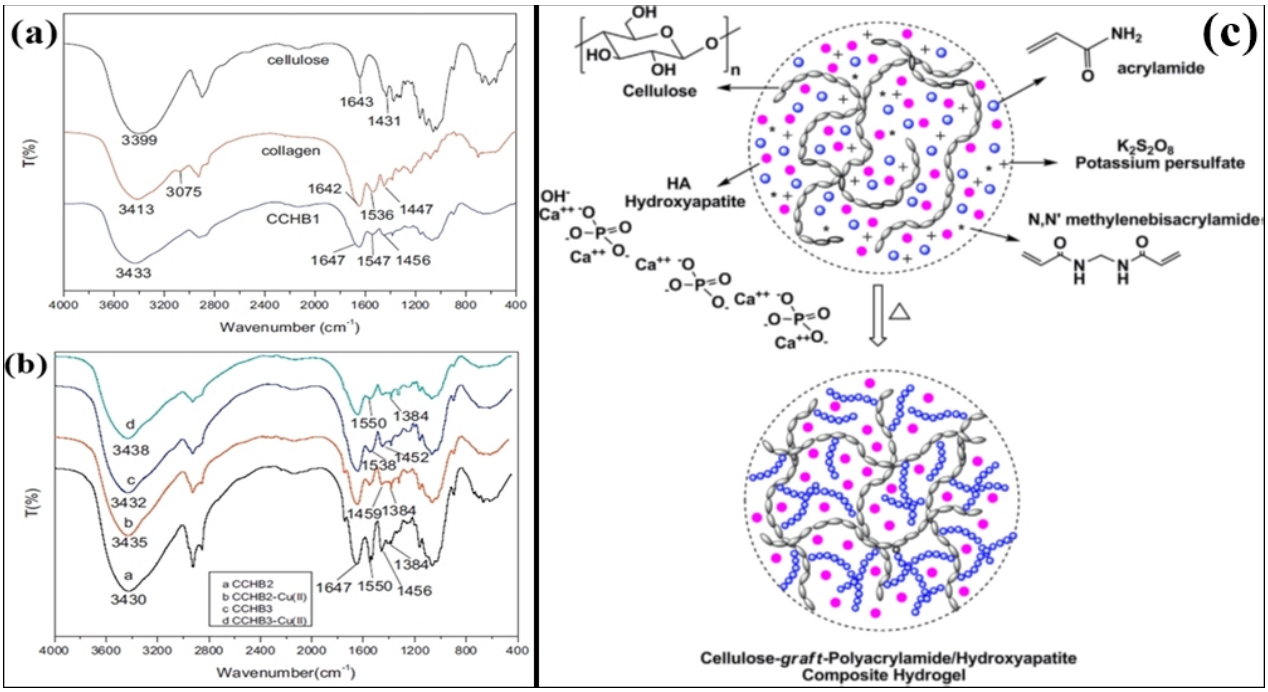


**Figure 8.** FTIR spectrum of **(a)** cellulose, collagen and cellulose-based collagen (cellulose & collagen is 1:1) hydrogel beads, **(b)** cellulose-based collagen (1:2) hydrogel beads (CCHB2), cellulose-based collagen (1:3) hydrogel beads (CCHB3) and Cu (II) ion adsorbed hydrogel beads [141]. Reprinted with permission from [141]. Copyright 2013 Elsevier, **(c)** possible mechanism for preparation of cellulose grafted polyacrylamide/hydroxyapatite hydrogel composite [142]. Reprinted with permission from [142]. Copyright 2013 Elsevier.

The FTIR spectrum of collagen, cellulose and cellulose-based collagen (cellulose & collagen: 1:1) hydrogel beads **(Figure 8a)** showed broad peaks at 3399 and 3413 $cm^{-1}$ were confirmed cellulose hydroxyl groups and amide group in collagen respectively. The broad peak of cellulose-based collagen (cellulose & collagen: 1:1) hydrogel beads (CCHB1) was due to the hydrogen bond at 3433 $cm^{-1}$. In the composite, the peak was broad and got shifted to a higher wavenumber and the peaks at 1536 and 1447 $cm^{-1}$ were because of amide groups of collagen. The FTIR spectrum of cellulose-based collagen (1:2) hydrogel beads (CCHB2), cellulose-based collagen (1:3) hydrogel

beads (CCHB3) and Cu (II) ion adsorbed hydrogels are represented in the **Figure 8b**. Because of the stretching vibration of O-H and N-H groups, CCHB2 and CCHB3 were represented a peak around 3430 $cm^{-1}$ but after adsorption peak was shifted to a higher frequency. The shifting of peaks has been also described as the removal of Cu (II) ions in the prepared hydrogel. After adsorption, O-H and N-H group peak was at around 3435 $cm^{-1}$. Peaks at 1550 and 1384 $cm^{-1}$ were due to N-H bending and C-N stretching in the CCHB2. In this study, researchers have prepared a blend ratio of collagen and cellulose, hence, cellulose cannot only be used as a backbone for hydrogel but also can be utilized as supporting material for the enhancement of the mechanical strength of hydrogel.

Wang et al., (2017) synthesised sugarcane cellulose supported bio-adsorbent for the elimination of heavy metals. The prepared bio-adsorbent was extremely efficient and environmentally sustainable [139]. Cellulose supported bio-adsorbent was utilized for removal of Cu (II), Zn (II) and Pb (II) metals ions and reported maximum adsorption tendency were 446.2, 363.3 and 558.9 mg $g^{-1}$ respectively. Carboxymethylcellulose and sugarcane bagasse cellulose were cross-linked with the help of epichlorohydrin, epichlorohydrin used as the crosslinking agent. The three-dimensional porous structure was shown by sugarcane cellulose-based bio-adsorbent. In another work, by suspension polymerization technique, cellulose-based polyacrylamide/hydroxyapatite composite was synthesized [142]. The prepared sample was examined for the effects on the adsorption while changing the time, pH, and concentration of Cu (II) ion solution. The maximum swelling and elimination capacity for Cu (II) metal ions was 5197 % per gram of hydrogel and 175 mg $g^{-1}$ respectively. **Figure 8c** shows the potential mechanism for the fabrication of cellulose-g-polyacrylamide/hydroxyapatite. Hydroxyapatite was used for the crosslinking of $OH^{-}$, amide groups of cellulose and acrylamide respectively. The cellulose as backbone and potassium

persulphate as initiator was utilized for the preparation of cellulose grafted hydrogel composite **(Figure 8c)**.

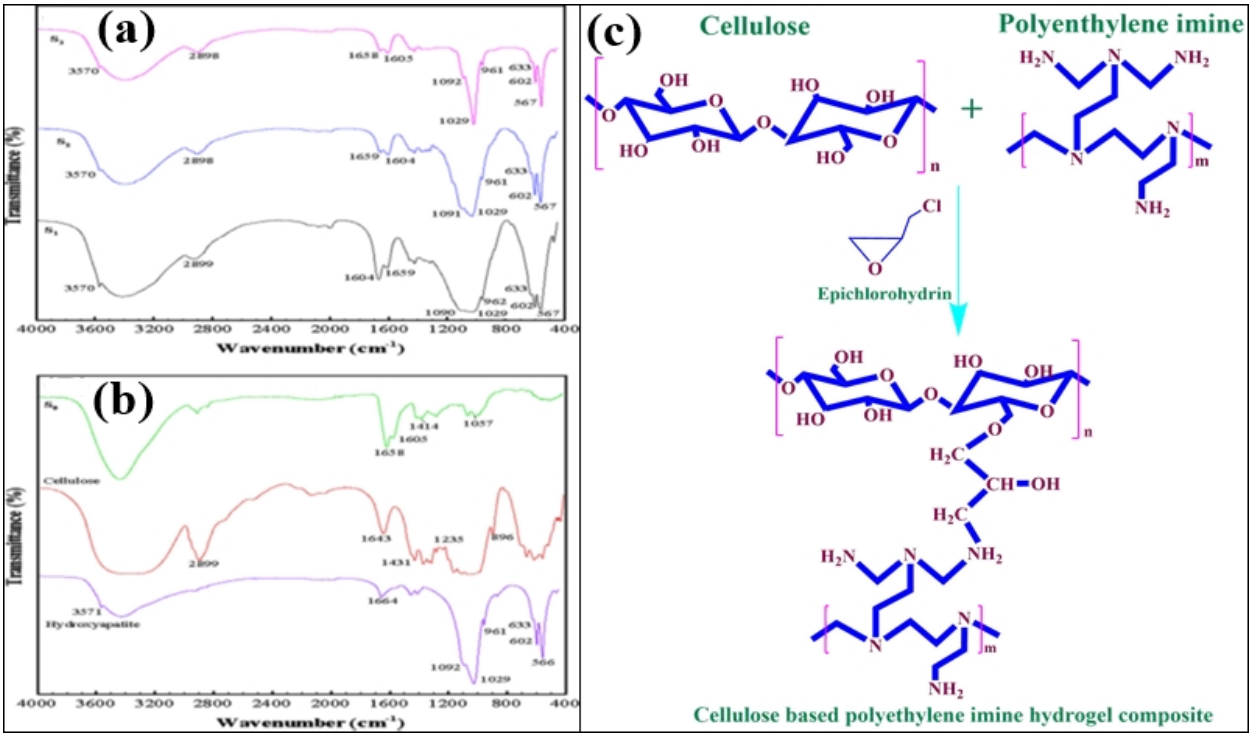


**Figure 9.** FTIR spectrum of **(a)** $S_1$ (hydroxyapatite, $Na_2HPO_4$ (0.09 mol $L^{-1}$) and $CaCl_2$ (0.15mol $L^{-1}$)), $S_2$ (hydroxyapatite, $Na_2HPO_4$ (0.18 mol $L^{-1}$) and $CaCl_2$ (0.31mol $L^{-1}$)), $S_3$ (hydroxyapatite, $Na_2HPO_4$ (0.54 mol $L^{-1}$) and $CaCl_2$ (0.92 mol $L^{-1}$)) and **(b)** $S_0$ (without hydroxyapatite), pure cellulose and hydroxyapatite [142]. Reprinted with permission from [142]. Copyright 2013 Elsevier, **(c)** possible mechanism for fabrication of cellulose supported polyethylene imine hydrogel composite [140]. Reprinted with permission from [140]. Copyright 2016 Springer.

The FTIR spectrums of pure cellulose, hydroxyapatite, and cellulose-g-polyacrylamide hydrogel ($S_0$) **(Figure 9b)** and different concentrations of hydroxyapatite in the cellulose-g-polyacrylamide hydrogel ($S_1$-$S_3$) **(Figure 9a)** are given in **Figure 9**. The broadband between 3000 and 3700 $cm^{-1}$ was due to hydroxyl groups stretching of cellulose, hydroxyapatite and water [157]. The broadband

at 896-1235 $cm^{-1}$ was because of C-O-C, a bridge stretching of polysaccharides. The phosphate groups present in the hydroxyapatite showed two different peaks at 602 and 566 $cm^{-1}$. After adding the hydroxyapatite in the hydrogel composite, the intensity of both peaks sharply increased, shown in the spectrum $S_1$-$S_3$. Peaks at 3570 $cm^{-1}$ and 633 $cm^{-1}$ confirmed the OH stretching/vibration and OH released respectively, these peaks were present in the pure hydroxyapatite as well in prepared hydrogels composite. Hence, cellulose-based hydrogels can be modified with carbonyl, amino and sulfo groups to improve adsorption. Cellulose can be modified into cellulose xanthate which is a novel approach to create super absorbing material. In cellulose xanthate, sulphide groups are responsible for more active sites for adsorption.

Ahmed et al., synthesized the cellulose supported hydrogel by grafting acrylamide with the help of glutaraldehyde as a crosslinker [143]. The prepared cellulose-based hydrogel was utilized for adsorption of Cu (II) and Cr (VI) from an aqueous solution. Reported higher adsorption percentages were 90.12 % and 94.2 % respectively. The grafting of acrylamide onto cellulose pulps with the help of potassium persulphate (initiator) and HCl (catalyst) followed by crosslinking and hydrolysis. Non-treated (pulp I) was decomposed in two steps but the other side treated (pulp (I) grafted acrylamide) was decomposed in three steps. In first decomposition step initial disintegration temperature (IDT) for treated (pulp (I) grafted acrylamide) and non-treated (pulp I) were detected 41.54 and 40.91ºC respectively. And final disintegration temperatures (FDT) were detected at 101.48 and 88.9 ºC respectively. In the second step of decomposition, initial temperatures were 195.13 and 201.3ºC and the final temperature was 323.68 and 394.55 ºC respectively. Maximum weight losses in the second step were 14.70% and 85.93% respectively [158]. And maximum weight loss of treated (pulp (I) grafted acrylamide) in the third step was 39.35%. Zhao et al. fabricated carboxymethylated cellulose-based chitosan physical hydrogel by

using the irradiation method [144]. Chitosan was mixed with carboxymethylated cellulose solution with the help of irradiation technique and after adding the chitosan, the removal tendency of the physical hydrogel was sharply enhanced. Mainly the prepared sample was utilized for the elimination of Cu (II), Cd (II) and Zn (II). The prepared hydrogel was shown excellent adsorption potential for heavy metal ions. It is a cost-effective approach in which cellulose is extracted from agricultural waste to create adsorbents for water refining applications. The uptake percentage for Cr (VI) was greater than Cu (II) which means Cr (VI) has smaller ionic radius than Cu (II) and it has more accessibility to attach with functional groups lying inside the matrix of the adsorbent. It also revealed from this study that the more the presence of carboxylic acid groups, the more will be the adsorption rate. The calculation of maximum equilibrium swelling of prepared samples by optimising the different parameters is a necessary part that provides more information needed to choose the best among alternatives.

Ge et al., prepared cellulose-based polyethyleneimine composite using cellulose as the backbone [140]. The polyethyleneimine was grafted onto cellulose with the help of an alkali/urea aqueous solvent in a step method. The prepared sample was used for the elimination of Cu (II) ions and higher removal efficiency was up to 285.7 mg $g^{-1}$. The synthesized composite was also utilized for adsorption of Pb (II), Cr (III), Ni (II) and Zn (II) ions and their removal efficiency were up to 248.2, 30.4, 112.2 and 148.4 mg $g^{-1}$ respectively. The potential mechanism for the fabrication of cellulose-based polyethylene imine composite hydrogel is presented in **Figure 9c**. The cellulose and polyethyleneimine were grafted using epichlorohydrin as a crosslinking agent. The stability and deformation resisting property of synthesized samples (cellulose hydrogel, cellulose-based polyethylene imine hydrogel composite) were compared as shown in **Figure 10a,b.** The mechanical property was enhanced with the incorporation of polyethyleneimine to cellulose

hydrogel. Furthermore, **Figure 10c,d** shows the comparison between SEM images of the cellulose-based hydrogel (2 wt%) and cellulose-based polyethylene imine hydrogel composite (cellulose 2 wt % and polyethyleneimine 5 wt %). The cellulose hydrogel had a porous structure with pore sizes ranging from 30 to 150 nm (**Figure 10c)**. The pore size was decreased to 10-50 nm after adding the polyethyleneimine into the cellulose chain (**Figure 10d**) because the polyethyleneimine molecule filled the interparticle space of the cellulose chain.

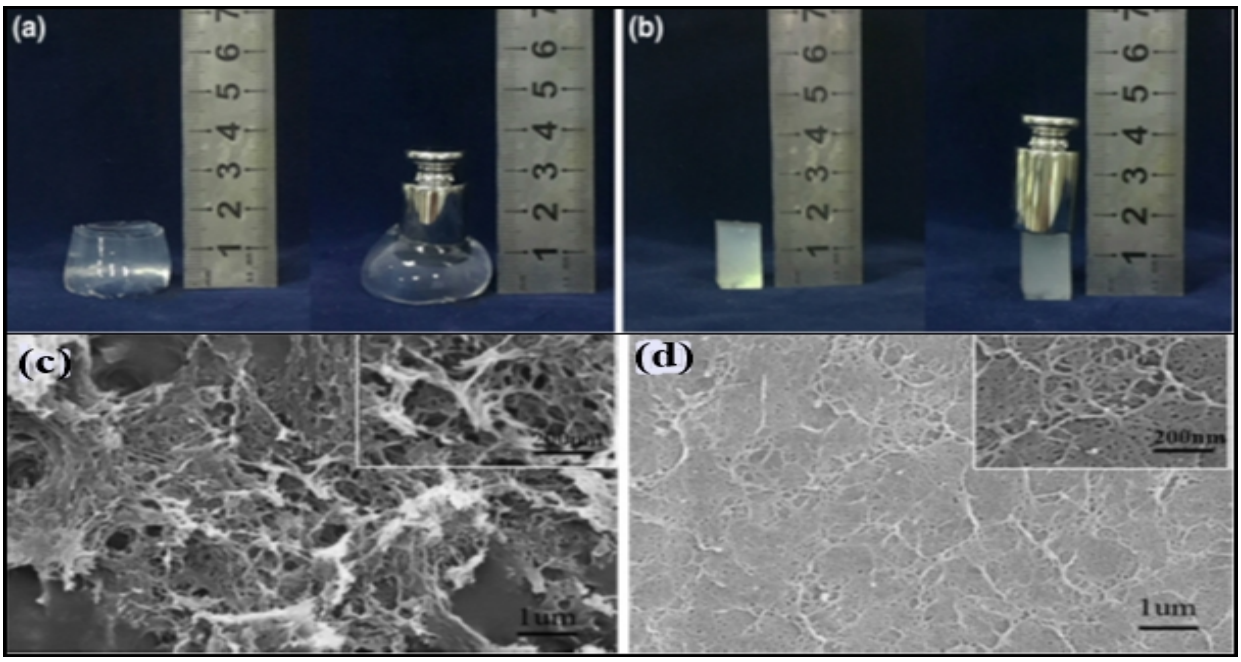


**Figure 10.** Representation of mechanical property of **(a)** cellulose based hydrogel (2 wt%) and **(b)** cellulose-based polyethylene imine hydrogel composite (cellulose 2 wt % and polyethylene imine 5 wt %) [140]. Reprinted with permission from [140]. Copyright 2016 Springer, SEM images of **(c)** cellulose supported hydrogel (2 wt %) and **(d)** cellulose-based polyethylene imine hydrogel composite (cellulose 2 wt % and polyethylene imine 5 wt %) [140]. Reprinted with permission from [140]. Copyright 2016 Springer.

Importantly, after adding the polyethyleneimine molecule into the cellulose chain, the removal tendency of hydrogel composite was sharply enhanced. In conclusion, a precooled alkali media was taken to synthesize hydrogel composite in which cellulose is selected as a skeleton and polyethyleneimine as a functional group. When compared to cellulose hydrogel, composite hydrogel demonstrated greater deformation resistance and stability after being modified with polyethyleneimine. Moreover, the adsorption capacity and equilibrium time varied with polyethyleneimine content. The best adsorption activity was reported at 20 % polyethyleneimine content for Cu (II).

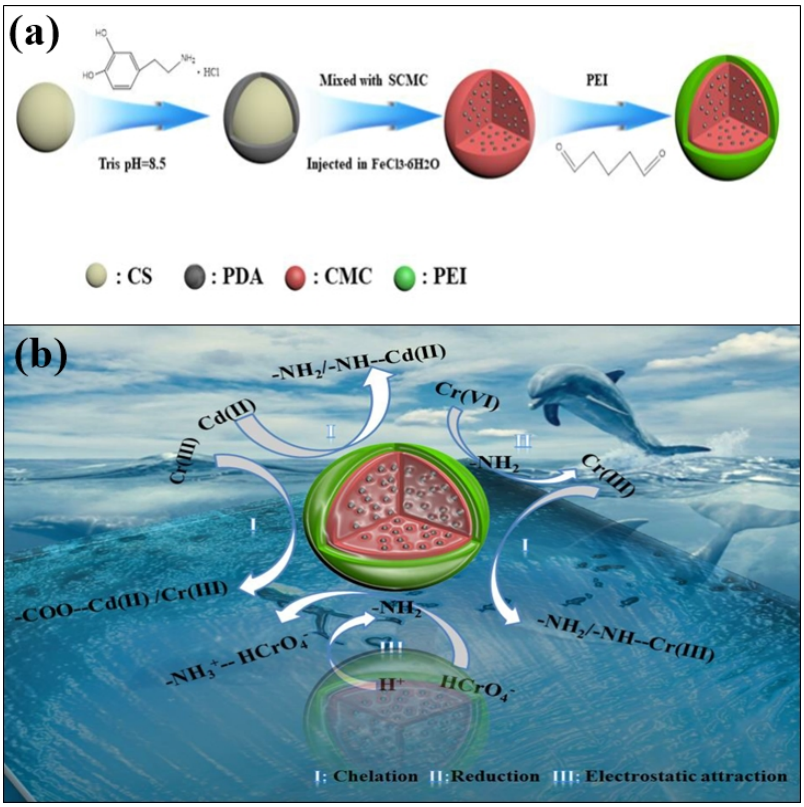


**Figure 11. (a)** Preparation of the carboxyl methylcellulose and chitosan supported nanostructured sorbent [136]. Reprinted with permission from [136]. Copyright 2020 Elsevier, **(b)** proposed

adsorption mechanism for Cr(VI) and Cd(II) [136]. Reprinted with permission from [136]. Copyright 2020 Elsevier.

Li et al., synthesized carboxymethyl cellulose and chitosan supported nanostructured sorbents [136]. In this study, sodium carboxymethyl cellulose (CMC) was doped in the chitosan (CS) and dopamine (DA) self-polymerized material with help of glutaraldehyde as a cross-linker. The prepared carboxymethyl cellulose and chitosan supported nanostructured sorbents were utilized for the adsorption of Cr (VI) and Cd (II) with the reported removal tendency of 470.0 mg $g^{-1}$ and 347.0 mg $g^{-1}$ respectively. **Figure 11a,b** show the preparation mechanism of the carboxyl methylcellulose and chitosan supported nanostructured sorbent and proposed adsorption mechanism for Cr(VI) and Cd(II).

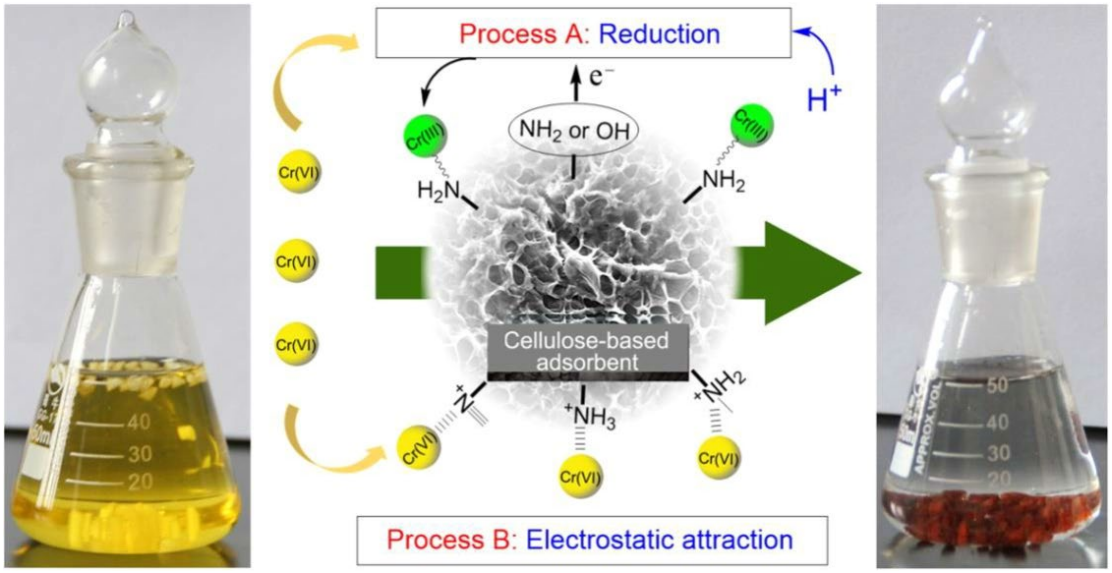


**Figure 12.** Proposed adsorption mechanism for Cr(VI) by synthesised adsorbent [133].

In another work, Liang et al., prepared a novel cellulose supported adsorbent with functional groups of quaternary ammonium and amino for adsorption of Cr (VI) from aqueous solution [133].

The reported higher removal tendency was 490.3 mg $g^{-1}$ for Cr (VI) ions. **Figure 12** describes the proposed adsorption mechanism for Cr(VI) by the synthesised adsorbent.

Liu et al. modified the cellulose beads by using TEMPO-mediated oxidation and bonded with Fe (III) for the preparation of Fe(III)-complexed carboxylated cellulose beads [134]. The prepared beads were used for the removal of bromide ions with the highest removal tendency of 1.22 mg $g^{-1}$.

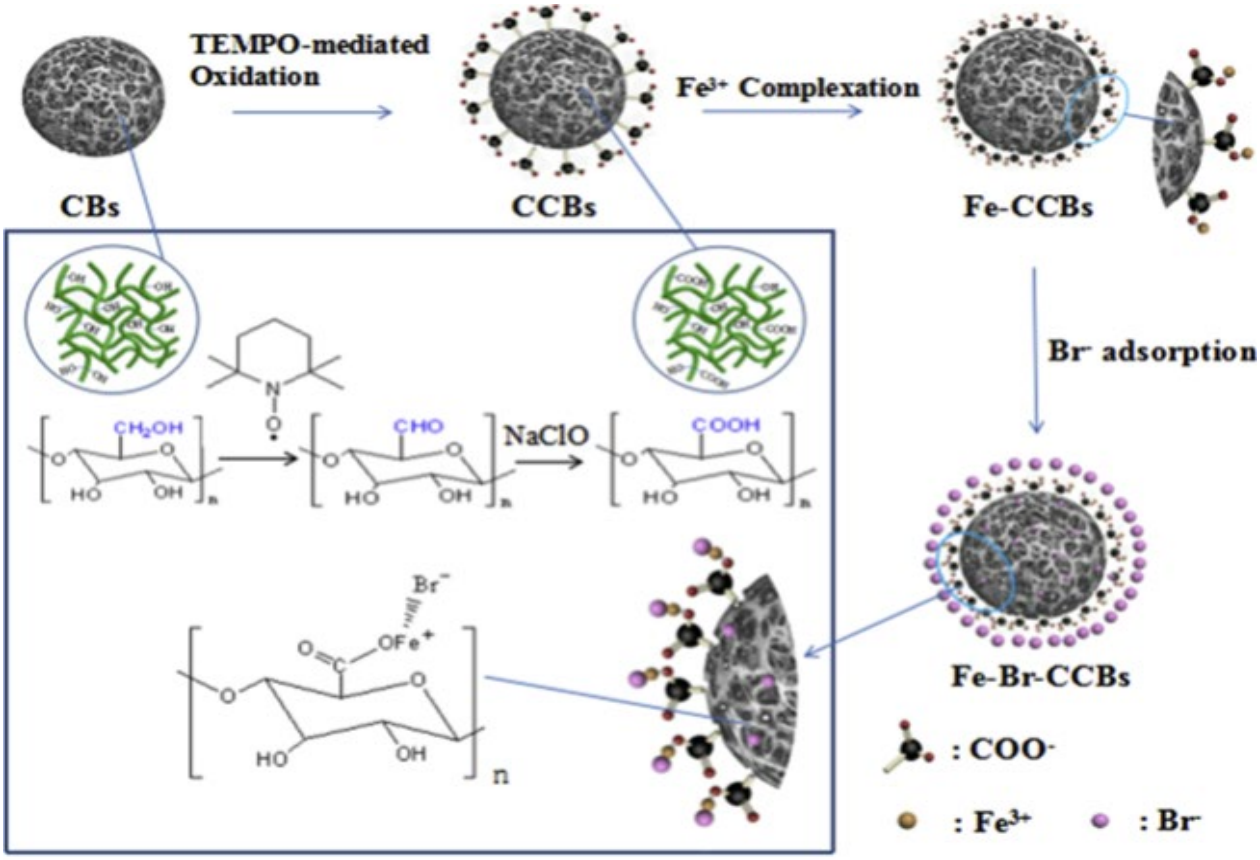


**Figure 13.** Representation of preparation process and adsorption of $Br^-$ by using Fe(III)-complexed carboxylated cellulose beads [134]. Reprinted with permission from [134]. Copyright 2020 Elsevier.

**Figure 13** explains the preparation process of the adsorbent and adsorption mechanism of bromide ions. Wu et al., synthesized the novel cellulose supported adsorbent by using microcrystalline cellulose, tetraethylenepentamine, bis(carboxymethyl) tri thiocarbonate and epichlorohydrin (crosslinker) [135]. The prepared adsorbent was used for adsorption of Cu (II), Pb (II) and Cr (VI). The diagram explained the preparation mechanism for synthesized cellulose supported adsorbent (**Figure14**). **Figure 15** shows the proposed adsorption mechanism for heavy metals (Cu (II), Pb (II) and Cr (VI)). Cellulose is poorly soluble in common solvents like water.

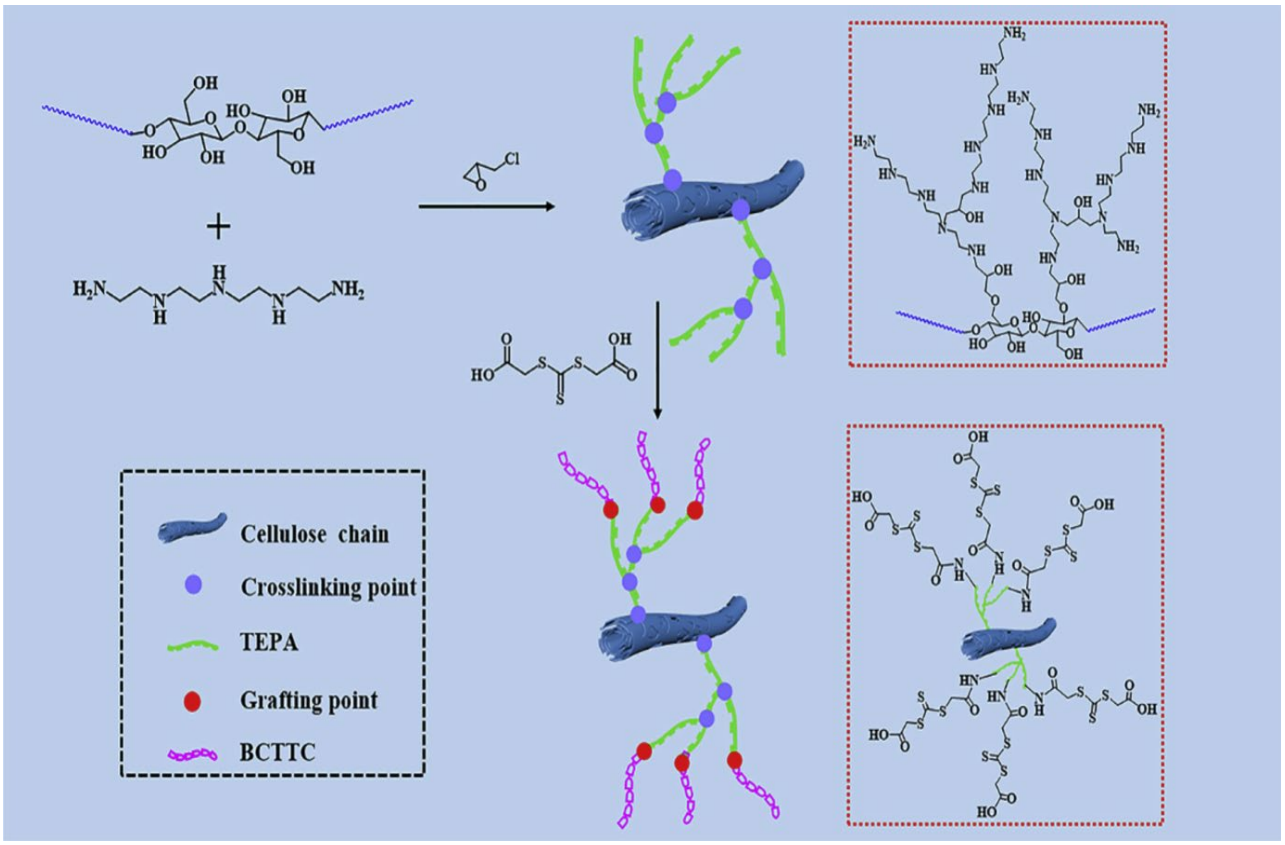


**Figure 14.** Figure shows the synthesis of cellulose-based adsorbent [135]. Reprinted with permission from [135]. Copyright 2020 Elsevier.

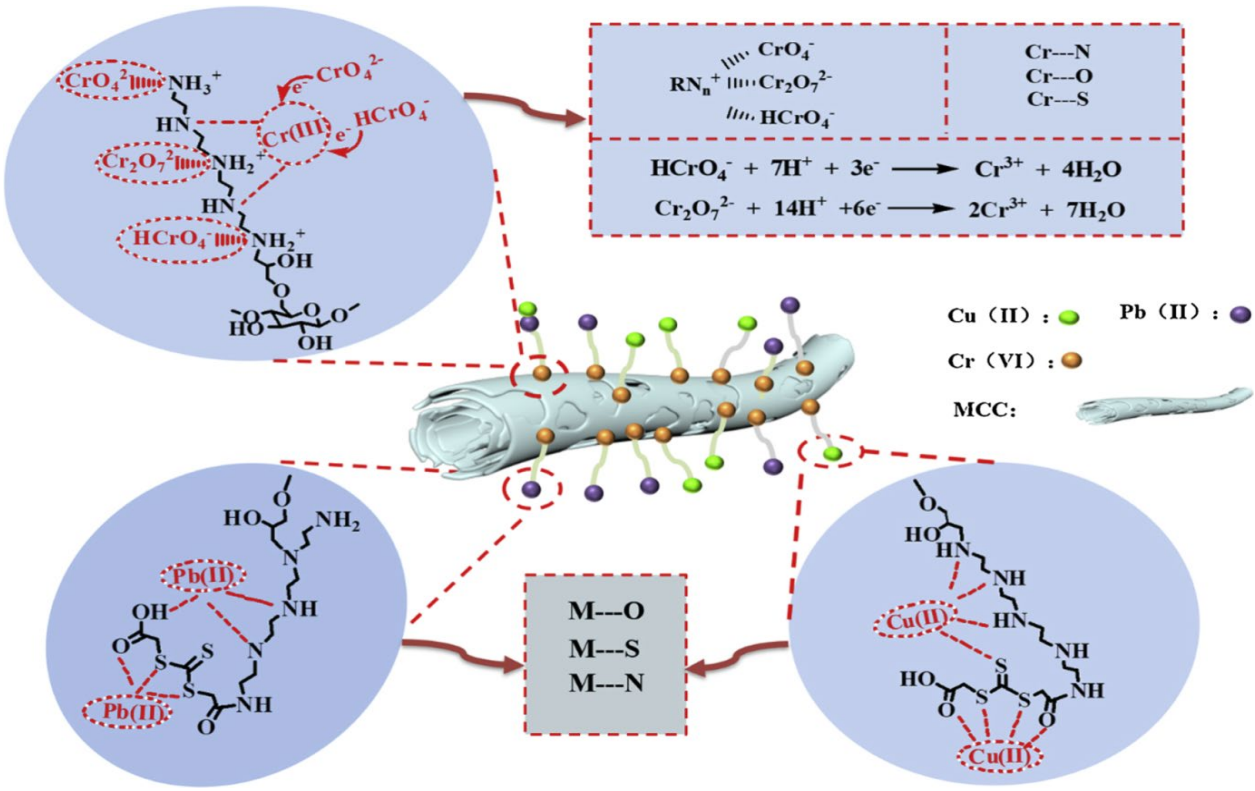


639

640 **Figure 15.** Show the proposed adsorption mechanism for Cu(II), Pb(II) and Cr(VI) [135].
641 Reprinted with permission from [135]. Copyright 2020 Elsevier.

642 A cellulose derivative called SCMC can be introduced as a dopant to create biopolymer beads for
643 adsorption. This is another scientific field in which the use of derivatives proved as the better
644 choice for the groundwork of super adsorbents. Saber-Samandari et al., synthesized carboxymethyl
645 cellulose-based poly (acrylic acid)/bentonite composite membrane [131]. In this study, poly
646 (acrylic acid) was grafted onto the carboxymethyl cellulose with the help of N, N'-
647 methylenebisacrylamide (crosslinker) and nanocomposite membrane were synthesized using silica
648 gel as an inorganic supporter and bentonite as the multifunctional crosslinker. The prepared
649 nanocomposite membranes were utilized for the elimination of heavy metal (Cd (II)) and organic
650 dye (Crystal violet). The maximum removal capacities for Cd (II) and crystal violet dye were 781
651 mg $g^{-1}$ and 546 mg $g^{-1}$.

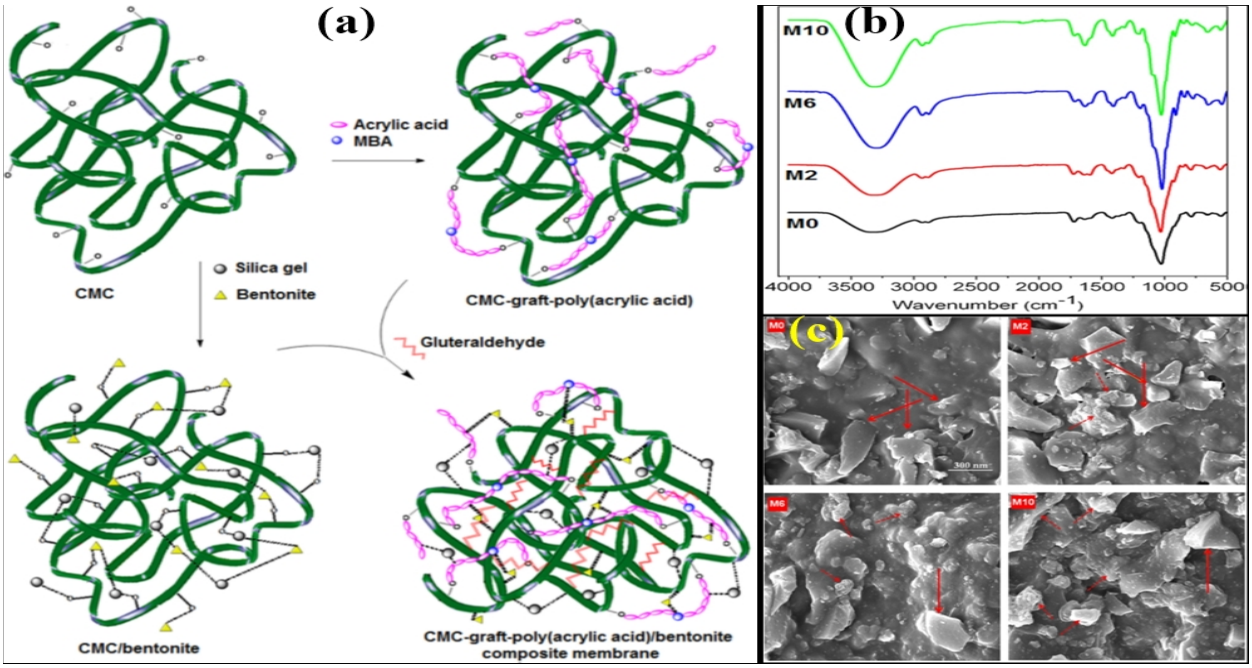


**Figure 16. (a)** Schematic representation for fabrication of carboxymethyl cellulose based poly (acrylic acid)/bentonite composite membrane [131]. Reprinted with permission from [131]. Copyright 2016 Elsevier, **(b)** FTIR spectrum of prepared grafted nanocomposite membranes. M0 (bentonite = 0), M2 (bentonite = 0.02 gm), M6 (bentonite = 0.06 gm) and M10 bentonite = 0.1 gm) [131]. Reprinted with permission from [131]. Copyright 2016 Elsevier, **(c)** SEM images of prepared nanocomposite membranes M0 (bentonite = 0), M2 (bentonite = 0.02 gm), M6 (bentonite = 0.06 gm) and M10 bentonite = 0.1 gm) [131]. Reprinted with permission from [131]. Copyright 2016 Elsevier.

**Figure 16a** shows a potential mechanism for prepared carboxymethyl cellulose-based poly(acrylic acid) composite, carboxymethyl cellulose-based bentonite composite and carboxymethyl cellulose-based poly (acrylic acid)/bentonite composite membrane. Carboxymethyl cellulose-based poly(acrylic acid) composite was prepared using acrylic acid as monomer and N, N'-methylenebisacrylamide as the crosslinking agent. Carboxymethyl cellulose-based bentonite

composite was synthesized using silica gel and bentonite. Carboxymethyl cellulose-based poly (acrylic acid)/bentonite composite membrane was fabricated using glutaraldehyde as the cross-linking agent through solvent evaporation **(Figure 16a)**.

The FTIR spectrum of prepared grafted nanocomposite membranes is represented in **Figure 16b**. The broad peak of hydroxyl groups at 3500 $cm^{-1}$ was shifted to 3450$cm^{-1}$, due to hydrogen bonding between -OH groups of carboxymethyl cellulose, silica gel, acrylic acid and bentonite. The peaks at 1082 and 2924 $cm^{-1}$ were confirmed the C-O-C in carboxymethyl cellulose and C-H stretching vibration in carboxymethyl cellulose-based poly(acrylic acid) composite respectively. The peaks at 1600-1700 $cm^{-1}$ corresponded to the stretching vibration in O-Si-O (silica gel) and Si-O-Si (bentonite). The stretching and bending vibration in Si-O (bentonite) were attributed to peaks at 1028 and 519 $cm^{-1}$ respectively. After adding the bentonite in the samples, the surface smoothness got diminished and small slab-like shapes were observed. The absence of bentonite in the M0 sample led to granular shapes which were because of silica gel **(Figure 16c)**. Bentonite has excellent adsorption properties, due to its high stability under reducing and oxidizing conditions, low water solubility, high surface area, better ease of use and low price tag. Because of these incomparable properties, bentonite can be used as an effective modifier in the case of creating biopolymer-based hydrogels for the active adsorption process.

The ion selectivity of an adsorbent depends upon the size of the ion and functional groups attached to the surface. Specifically, the C=N group on the adsorbent surface is responsible for the high selectivity of $Hg^{2+}$ [159]. C=N behave as a soft basic ligand for interaction with soft acid $Hg^{2+}$ as per acid-base theory. Furthermore, the chemical hardness of $Hg^{2+}$ is much lower than that of $Cd^{2+}$, so the soft base binds preferentially to $Hg^{2+}$. Cellulose-based adsorbent performance is mostly determined by the wastewater's properties [160]. Mainly, adsorption processes depend upon the

pH of the adsorbate solution. For instance, various amino-modified cellulose-based hydrogels are suggested to be promising metal and other pollution adsorbents. The amino groups, which have limited effectiveness in pollutants absorption at low pH ranges because of amino groups protonation. Aside from pH, other variables like contact time, initial concentration, temperature, adsorbent dose, etc. can affect the adsorption process. It is challenging to predict the prospective uses of cellulose-based adsorbents in wastewater treatment and their removal effectiveness in real industrial effluents due to the lack of full-scale investigations. A few cellulosic materials have demonstrated their ability to remove pollutants without any changes, however, their removal capabilities can be enhanced by chemical modifications, degree of modification and chemical activation affecting the adsorption in the great way [161].

### 3.4. Regeneration of cellulose-based hydrogels

Regeneration of cellulose adsorbent is essential to recover its original adsorption capability. It permits the recovery of cellulose adsorbent by removing the pollutants and returning the cellulose adsorbent to the process of adsorption [162]. The pollutants (organic and inorganic) can be efficiently extracted from the pollutant loaded cellulose adsorbent with the help of dilute acids (like diluted hydrochloric, nitric and sulfuric acids) [163]. Desorption can be accomplished by employing an acidic solution, sorption process is extremely sensitive to pH, change in the pH can reverse the sorption [70]. Tan et al., prepared the hydrogel made up of N-isopropylacrylamide, acrylic acid and carboxymethyl cellulose for U(VI) removal [164], desorption of U(VI) was monitored by immersing hydrogel in 0.1 mol $L^{-1}$ of $HNO_3$ solution at various temperatures, UV-spectrophotometry was used to determine the remaining U(VI) concentration in solution, after five cycles of adsorption-desorption, the experiments demonstrated that the resolution rate remained at around 77.74%. [164].

### 3.5. Biodegradation of cellulose-based hydrogels

The potential of hydrogels to degrade in both aerobic and anaerobic environments is known to be the most influential property. Many methods have been used to change the chemical and physical properties of natural polymers with different monomers appropriate for specific industrial applications. Feng et al. was synthesized the superabsorbent polymer with the help of cellulose from flax shive, potassium persulphate, N, N'-methylenebisacrylamide and microwave irradiation [165]. The prepared sample had good biodegradability by the soil composting method. The superabsorbent polymer was biologically degraded up to 40 % in 54 days at 40 °C. In another work, using yeast as a foaming agent, a novel polyvinyl alcohol/carboxymethyl cellulose/yeast double degradable hydrogel was synthesized [166]. The addition of yeast encouraged the hydrogel biodegradability and improved the degradation rate of polyvinyl alcohol in the prepared hydrogel with the highest degradation rate of 45 ± 2.8%. So, due to biocompatibility and biodegradability, cellulose-based hydrogels are a promising material for several industrial as well as biomedical applications [167].

### 3.6 Photocatalytic activities of cellulose-based nanostructured photocatalyst

Photocatalysts are another important class of materials that are being used for water remediation applications[168–172]. The use of nanostructured photocatalyst in co-junction with cellulose-based materials supports the creation of novel bio-hybrid materials for a variety of applications, notably renewable energy and water purification. The biocompatibility and strong hydrophilicity of cellulose result in good compatibility [173], the presence of electron-rich hydroxyl groups in cellulose contributes to photocatalyst interaction. Because of the synergistic behaviour of specific cellulose supported hydrogels and photocatalyst nanoparticles, the creation of bio-hybrid

nanostructured is gaining a lot of attention [59,174]. **Table 3** represents the recently developed cellulose supported photocatalyst composited and their utilization in wastewater remediation.

**Table 3.** Photocatalytic activity of cellulose supported photocatalyst composites.

| Sr. No. | Composite | Pollutant | Removal % | Reaction Time | References |
|---|---|---|---|---|---|
| **1.** | Cellulose/Graphene oxide/$TiO_2$ hydrogel photocatalyst | Methylene blue | 93% | 120 min | [175] |
| **2.** | Cellulose/ β-FeOOH composite hydrogel | Methylene blue | 99.89% | 30 min | [176] |
| **3.** | Ag/AgCl@Al-carboxymethyl cellulose composite | Rhodamine B | 98% | 60 min | [177] |
| **4.** | AgCl@Fe-carboxymethyl cellulose composite | Rhodamine B | 87% | 60 min | [177] |
| **5.** | $ZnFe_2O_4$@methyl cellulose composite | Metronidazole | 92.65% and 71.12% in synthetic and real samples | - | [178] |

## 4. Conclusion and future perspectives

On earth, Cellulose is the utmost abundant organic polymer and is one of the key component of plant cell walls that provides strength to plant cell walls [179-181]. The applications of cellulose

in everyday life are growing extensively replacing synthetic materials. In particular, cellulosic biomass-based sustainable hydrogels have earned significant care in the area of contaminated water remediation because of their exceptional characteristics like high adsorption tendency, rapid kinetics, and reusability. Aside from these characteristics, hydrogels fabricated from cellulose have low mechanical stability. The used technique for the fabrication of hydrogels fabricated from cellulose is crucial in resolving mechanical stability. This review represents the recent development in hydrogels fabricated from cellulose for wastewater remediation, which includes the comparative study of different hydrogels fabricated from cellulose to remove toxins from aqueous solutions. The present discussion can provide novel ideas in the area of hydrogels fabricated from cellulose for wastewater remediation. The following are the gaps that must be addressed in future works:

- Modification of cellulose and hydrogels fabricated from cellulose should be exploited to improve the adsorption capability and adsorption rate.
- Necessary to investigate the efficiency of hydrogels fabricated from cellulose for the treatment of industrial pollutants containing different contaminants.
- The economic sustainability of adsorbents is determined by the reusability of hydrogels, detailed research on the regeneration capabilities of hydrogels fabricated from cellulose in different cycles should be conducted to determine their reusability.
- The majority of the research focused on treatments of lab-based wastewater rather than genuine industrial wastewater.
- Most significant limitation throughout the research works is lack of clarity and poor information on the adsorption mechanism. More experimental and theoretical study are

needed to understand adsorption mechanisms that can potentially unlock and find the most effective technique.

- It is critical to investigate the possibility of increasing the mechanical durability of cellulose-based hydrogels by increasing self-healing ability.
- Key parameters, planned formulation and optimum synthesis can overcome problems and inadequacies such as lower resistivity and mechanical strength.

**Acknowledgement**

Sourbh Thakur acknowledges the financial support from the ID-UB program, Silesian University of Technology, Gliwice, Poland.

**Author Contributions**

Original draft writing, A.V., S.T.; writing, review and editing, S.T., V.K.T., V.K., X.J.Y., F.C.; supervision, S.T., V.K.T. All authors have read and agreed to the published version of the manuscript.

**References**

[1] Ates B, Koytepe S, Ulu A, Gurses C, Thakur VK. Chemistry, Structures, and Advanced Applications of Nanocomposites from Biorenewable Resources. Chem Rev 2020;120:9304–62. https://doi.org/10.1021/acs.chemrev.9b00553.

[2] Siwal SS, Zhang Q, Devi N, Saini AK, Saini V, Pareek B, et al. Recovery processes of sustainable energy using different biomass and wastes. Renewable and Sustainable Energy Reviews 2021;150:111483. https://doi.org/10.1016/j.rser.2021.111483.

[3] K. Rana A, Kumar Thakur V. The bright side of cellulosic hibiscus sabdariffa fibres: towards sustainable materials from the macro- to nano-scale. Materials Advances 2021. https://doi.org/10.1039/D1MA00429H.

[4] Voicu SI, Thakur VK. Aminopropyltriethoxysilane as a linker for cellulose-based functional materials: New horizons and future challenges. Current Opinion in Green and Sustainable Chemistry 2021;30:100480. https://doi.org/10.1016/j.cogsc.2021.100480.

[5] Usmani Z, Sharma M, Awasthi AK, Sharma GD, Cysneiros D, Nayak SC, et al. Minimizing hazardous impact of food waste in a circular economy – Advances in resource recovery through green strategies. Journal of Hazardous Materials 2021;416:126154. https://doi.org/10.1016/j.jhazmat.2021.126154.

[6] Zielińska D, Rydzkowski T, Thakur VK, Borysiak S. Enzymatic engineering of nanometric cellulose for sustainable polypropylene nanocomposites. Industrial Crops and Products 2021;161:113188. https://doi.org/10.1016/j.indcrop.2020.113188.

[7] Hernández-Cocoletzi H, Salinas RA, Águila-Almanza E, Rubio-Rosas E, Chai WS, Chew KW, et al. Natural hydroxyapatite from fishbone waste for the rapid adsorption of heavy metals of aqueous effluent. Environmental Technology & Innovation 2020;20:101109.

[8] Chai WS, Cheah KH, Meng H, Li G. Experimental and analytical study on electrolytic decomposition of HAN-water solution using graphite electrodes. Journal of Molecular Liquids 2019;293:111496.

[9] Lee P-X, Liu B-L, Show PL, Ooi CW, Chai WS, Munawaroh HSH, et al. Removal of calcium ions from aqueous solution by bovine serum albumin (BSA)-modified nanofiber membrane: Dynamic adsorption performance and breakthrough analysis. Biochemical Engineering Journal 2021;171:108016.

[10] Chai WS, Tan WG, Munawaroh HSH, Gupta VK, Ho S-H, Show PL. Multifaceted roles of microalgae in the application of wastewater biotreatment: A review. Environmental Pollution 2020:116236.

[11] Rathod H. Algae based wastewater treatment. A Seminar Report of Master of Technology in Civil Engineering. Roorkee, Uttarakhand, India, 2014.

[12] Chai WS, Cheun JY, Kumar PS, Mubashir M, Majeed Z, Banat F, et al. A review on conventional and novel materials towards heavy metal adsorption in wastewater treatment application. Journal of Cleaner Production 2021:126589.

[13] Danish M, Anirudh PV, Karunakaran C, Rajamohan V, Mathew AT, Koziol K, et al. 4D printed stereolithography printed plant-based sustainable polymers: Preliminary investigation and optimization. Journal of Applied Polymer Science 2021;138:50903. https://doi.org/10.1002/app.50903.

[14] Daminabo SC, Goel S, Grammatikos SA, Nezhad HY, Thakur VK. Fused deposition modeling-based additive manufacturing (3D printing): techniques for polymer material systems. Materials Today Chemistry 2020;16:100248. https://doi.org/10.1016/j.mtchem.2020.100248.

[15] Joshi S, Rawat K, C K, Rajamohan V, Mathew AT, Koziol K, et al. 4D printing of materials for the future: Opportunities and challenges. Applied Materials Today 2020;18:100490. https://doi.org/10.1016/j.apmt.2019.100490.

[16] Chai WS, Sun D, Cheah KH, Li G, Meng H. Co-Electrolysis-Assisted Decomposition of Hydroxylammonium Nitrate–Fuel Mixtures Using Stainless Steel–Platinum Electrodes. ACS Omega 2020;5:19525–32.

828 [17] Guo Y, Bae J, Fang Z, Li P, Zhao F, Yu G. Hydrogels and hydrogel-derived materials for
829 energy and water sustainability. Chemical Reviews 2020;120:7642–707.
830 [18] Su M, Liu Y, Li S, Fang Z, He B, Zhang Y, et al. A rubber-like, underwater superoleophobic
831 hydrogel for efficient oil/water separation. Chemical Engineering Journal 2019;361:364–72.
832 [19] Sharma B, Thakur S, Mamba G, Prateek, Gupta RK, Gupta VK, et al. Titania modified gum
833 tragacanth based hydrogel nanocomposite for water remediation. Journal of Environmental
834 Chemical Engineering 2020:104608. https://doi.org/10.1016/j.jece.2020.104608.
835 [20] Thakur S, Sharma B, Verma A, Chaudhary J, Tamulevicius S, Thakur VK. Recent
836 approaches in guar gum hydrogel synthesis for water purification. International Journal of
837 Polymer Analysis and Characterization 2018;23:621–32.
838 https://doi.org/10.1080/1023666X.2018.1488661.
839 [21] Hoffman AS. Hydrogels for biomedical applications. Advanced Drug Delivery Reviews
840 2012;64:18–23.
841 [22] Kulal P, Badalamoole V. Efficient removal of dyes and heavy metal ions from waste water
842 using Gum ghatti–graft–poly (4-acryloylmorpholine) hydrogel incorporated with magnetite
843 nanoparticles. Journal of Environmental Chemical Engineering 2020:104207.
844 [23] Mohammadinejad R, Maleki H, Larrañeta E, Fajardo AR, Nik AB, Shavandi A, et al. Status
845 and future scope of plant-based green hydrogels in biomedical engineering. Applied
846 Materials Today 2019;16:213–46. https://doi.org/10.1016/j.apmt.2019.04.010.
847 [24] Thakur S, Govender PP, Mamo MA, Tamulevicius S, Thakur VK. Recent progress in gelatin
848 hydrogel nanocomposites for water purification and beyond. Vacuum 2017;146:396–408.
849 https://doi.org/10.1016/j.vacuum.2017.05.032.

[25] Thakur S, Chaudhary J, Kumar V, Thakur VK. Progress in pectin based hydrogels for water purification: Trends and challenges. Journal of Environmental Management 2019;238:210–23. https://doi.org/10.1016/j.jenvman.2019.03.002.

[26] Chen C, Wang L, Huang Y. Crosslinking of the electrospun polyethylene glycol/cellulose acetate composite fibers as shape-stabilized phase change materials. Materials Letters 2009;63:569–71.

[27] Ijaz QA, Abbas N, Arshad MS, Hussain A, Shahiq-uz-Zaman, Javaid Z. Synthesis and evaluation of pH dependent polyethylene glycol-co-acrylic acid hydrogels for controlled release of venlafaxine HCl. Journal of Drug Delivery Science and Technology 2018;43:221–32. https://doi.org/10.1016/j.jddst.2017.10.010.

[28] Lim HJ, Khan Z, Lu X, Perera TH, Wilems TS, Ravivarapu KT, et al. Mechanical stabilization of proteolytically degradable polyethylene glycol dimethacrylate hydrogels through peptide interaction. Acta Biomaterialia 2018;71:271–8. https://doi.org/10.1016/j.actbio.2018.03.001.

[29] Numata Y, Kono H, Tsuji M, Tajima K. Structural and mechanical characterization of bacterial cellulose–polyethylene glycol diacrylate composite gels. Carbohydrate Polymers 2017;173:67–76. https://doi.org/10.1016/j.carbpol.2017.05.077.

[30] Thakur VK, Thakur MK. Recent Advances in Graft Copolymerization and Applications of Chitosan: A Review. ACS Sustainable Chem Eng 2014; 2:2637–52. https://doi.org/10.1021/sc500634p.

[31] Sharma B, Thakur S, Trache D, Yazdani Nezhad H, Thakur VK. Microwave-Assisted Rapid Synthesis of Reduced Graphene Oxide-Based Gum Tragacanth Hydrogel Nanocomposite for Heavy Metal Ions Adsorption. Nanomaterials 2020;10:1616.

873 [32] Chaudhary J, Thakur S, Mamba G, Prateek, Gupta RK, Thakur VK. Hydrogel of Gelatin in
874 the Presence of Graphite for the Adsorption of Dye: Towards the Concept for Water
875 Purification. Journal of Environmental Chemical Engineering 2020:104762.
876 https://doi.org/10.1016/j.jece.2020.104762.
877 [33] Dehshahri A, Kumar A, Madamsetty VS, Uzieliene I, Tavakol S, Azedi F, et al. New
878 Horizons in Hydrogels for Methotrexate Delivery. Gels 2021;7:2.
879 https://doi.org/10.3390/gels7010002.
880 [34] Khan M, Lo IM. A holistic review of hydrogel applications in the adsorptive removal of
881 aqueous pollutants: Recent progress, challenges, and perspectives. Water Research
882 2016;106:259–71.
883 [35] Dulta K, Ağçeli GK, Chauhan P, Jasrotia R, Chauhan PK. A Novel Approach of Synthesis
884 Zinc Oxide Nanoparticles by Bergenia ciliata Rhizome Extract: Antibacterial and Anticancer
885 Potential. Journal of Inorganic and Organometallic Polymers and Materials 2020:1–11.
886 [36] Chaudhary J, Thakur S, Sharma M, Gupta VK, Thakur VK. Development of Biodegradable
887 Agar-Agar/Gelatin-Based Superabsorbent Hydrogel as an Efficient Moisture-Retaining
888 Agent. Biomolecules 2020;10:939. https://doi.org/10.3390/biom10060939.
889 [37] Agate S, Joyce M, Lucia L, Pal L. Cellulose and Nanocellulose-Based Flexible-Hybrid
890 Printed Electronics and Conductive Composites – A Review. Carbohydrate Polymers n.d.
891 https://doi.org/10.1016/j.carbpol.2018.06.045.
892 [38] Corsi I, Winther-Nielsen M, Sethi R, Punta C, Della Torre C, Libralato G, et al. Ecofriendly
893 nanotechnologies and nanomaterials for environmental applications: Key issue and
894 consensus recommendations for sustainable and ecosafe nanoremediation. Ecotoxicology
895 and Environmental Safety 2018;154:237–44. https://doi.org/10.1016/j.ecoenv.2018.02.037.

[39] Thakur S, Govender PP, Mamo MA, Tamulevicius S, Mishra YK, Thakur VK. Progress in lignin hydrogels and nanocomposites for water purification: Future perspectives. Vacuum 2017;146:342–55. https://doi.org/10.1016/j.vacuum.2017.08.011.

[40] Nebot VJ, Armengol J, Smets J, Prieto SF, Escuder B, Miravet JF. Molecular hydrogels from bolaform amino acid derivatives: A structure–properties study based on the thermodynamics of gel solubilization. Chemistry-A European Journal 2012;18:4063–72.

[41] Yang J, Li J. Self-assembled cellulose materials for biomedicine: A review. Carbohydrate Polymers 2018;181:264–74. https://doi.org/10.1016/j.carbpol.2017.10.067.

[42] Thakur S, Sharma B, Verma A, Chaudhary J, Tamulevicius S, Thakur VK. Recent progress in sodium alginate based sustainable hydrogels for environmental applications. Journal of Cleaner Production 2018;198:143–59. https://doi.org/10.1016/j.jclepro.2018.06.259.

[43] Thakur VK, Thakur MK. Recent advances in green hydrogels from lignin: a review. International Journal of Biological Macromolecules 2015;72:834–47. https://doi.org/10.1016/j.ijbiomac.2014.09.044.

[44] Lapwanit S, Sooksimuang T, Trakulsujaritchok T. Adsorptive removal of cationic methylene blue dye by kappa-carrageenan/poly (glycidyl methacrylate) hydrogel beads: Preparation and characterization. Journal of Environmental Chemical Engineering 2018;6:6221–30.

[45] Hasan MN, Shenashen MA, Hasan MM, Znad H, Awual MR. Assessing of cesium removal from wastewater using functionalized wood cellulosic adsorbent. Chemosphere 2021;270:128668.

[46] Verma A, Thakur S, Goel G, Raj J, Gupta VK, Roberts D, et al. Bio-based Sustainable Aerogels: New Sensation in CO2 Capture. Current Research in Green and Sustainable Chemistry 2020:100027.

[47] Verma A, Thakur S, Mamba G, Gupta RK, Thakur P, Thakur VK. Graphite modified sodium alginate hydrogel composite for efficient removal of malachite green dye. International Journal of Biological Macromolecules 2020;148:1130–9.

[48] Chen X, Li Z, He N, Zheng Y, Li H, Wang H, et al. Nitrogen and phosphorus removal from anaerobically digested wastewater by microalgae cultured in a novel membrane photobioreactor. Biotechnology for Biofuels 2018;11:1–11.

[49] Lin C-Y, Chai WS, Lay C-H, Chen C-C, Lee C-Y, Show PL. Optimization of Hydrolysis-Acidogenesis Phase of Swine Manure for Biogas Production Using Two-Stage Anaerobic Fermentation. Processes 2021;9:1324.

[50] Das A, Adhikari S, Kundu P. Bioremediation of wastewater using microalgae. Environmental Biotechnology For Soil and Wastewater Implications on Ecosystems, Springer; 2019, p. 55–60.

[51] Fu L-H, Qi C, Ma M-G, Wan P. Multifunctional cellulose-based hydrogels for biomedical applications. Journal of Materials Chemistry B 2019;7:1541–62.

[52] He J, Ni F, Cui A, Chen X, Deng S, Shen F, et al. New insight into adsorption and co-adsorption of arsenic and tetracycline using a Y-immobilized graphene oxide-alginate hydrogel: Adsorption behaviours and mechanisms. Science of The Total Environment 2020;701:134363.

[53] Thakur S, Chaudhary J, Sharma B, Verma A, Tamulevicius S, Thakur VK. Sustainability of Bioplastics: Opportunities and Challenges. Current Opinion in Green and Sustainable Chemistry 2018.

[54] Thakur S, Verma A, Sharma B, Chaudhary J, Tamulevicius S, Thakur VK. Recent developments in recycling of polystyrene based plastics. Current Opinion in Green and Sustainable Chemistry 2018.

[55] Kumar AC, Erothu H. Synthetic Polymer Hydrogels. Biomedical Applications of Polymeric Materials and Composites 2016.

[56] De France KJ, Chan KJ, Cranston ED, Hoare T. Enhanced mechanical properties in cellulose nanocrystal–poly (oligoethylene glycol methacrylate) injectable nanocomposite hydrogels through control of physical and chemical cross-linking. Biomacromolecules 2016;17:649–60.

[57] Déléris I, Wallecan J. Relationship between processing history and functionality recovery after rehydration of dried cellulose-based suspensions: A critical review. Advances in Colloid and Interface Science 2017;246:1–12. https://doi.org/10.1016/j.cis.2017.06.013.

[58] Guilherme MR, Aouada FA, Fajardo AR, Martins AF, Paulino AT, Davi MFT, et al. Superabsorbent hydrogels based on polysaccharides for application in agriculture as soil conditioner and nutrient carrier: A review. European Polymer Journal 2015;72:365–85. https://doi.org/10.1016/j.eurpolymj.2015.04.017.

[59] Mohamed MA, Abd Mutalib M, Mohd Hir ZA, M. Zain MF, Mohamad AB, Jeffery Minggu L, et al. An overview on cellulose-based material in tailoring bio-hybrid nanostructured photocatalysts for water treatment and renewable energy applications. International Journal of Biological Macromolecules 2017;103:1232–56. https://doi.org/10.1016/j.ijbiomac.2017.05.181.

[60] Zhou A, Chen W, Liao L, Xie P, Zhang TC, Wu X, et al. Comparative adsorption of emerging contaminants in water by functional designed magnetic poly (N-

963 isopropylacrylamide)/chitosan hydrogels. Science of the Total Environment 2019;671:377–
964 87.
965 [61] Gaharwar AK, Peppas NA, Khademhosseini A. Nanocomposite hydrogels for biomedical
966 applications. Biotechnology and Bioengineering 2014;111:441–53.
967 [62] Nechyporchuk O, Belgacem MN, Bras J. Production of cellulose nanofibrils: A review of
968 recent advances. Industrial Crops and Products 2016;93:2–25.
969 https://doi.org/10.1016/j.indcrop.2016.02.016.
970 [63] Wang S, Lu A, Zhang L. Recent advances in regenerated cellulose materials. Progress in
971 Polymer Science 2016;53:169–206. https://doi.org/10.1016/j.progpolymsci.2015.07.003.
972 [64] Singh NB, Nagpal G, Agrawal S, Rachna. Water purification by using Adsorbents: A
973 Review. Environmental Technology & Innovation 2018;11:187–240.
974 https://doi.org/10.1016/j.eti.2018.05.006.
975 [65] Mohammed N, Grishkewich N, Tam KC. Cellulose nanomaterials: promising sustainable
976 nanomaterials for application in water/wastewater treatment processes. Environmental
977 Science: Nano 2018;5:623–58.
978 [66] Kabir SF, Sikdar PP, Haque B, Bhuiyan MR, Ali A, Islam MN. Cellulose-based hydrogel
979 materials: chemistry, properties and their prospective applications. Progress in Biomaterials
980 2018;7:153–74.
981 [67] Rana AK, Mishra YK, Gupta VK, Thakur VK. Sustainable materials in the removal of
982 pesticides from contaminated water: Perspective on macro to nanoscale cellulose. Science of
983 The Total Environment 2021;797:149129. https://doi.org/10.1016/j.scitotenv.2021.149129.
984 [68] Usmani Z, Sharma M, Lukk T, Karpichev Y, Thakur VK, Kumar V, et al. Developments in
985 enzyme and microalgae based biotechniques to remediate micropollutants from aqueous

systems—A review. Critical Reviews in Environmental Science and Technology 2020;0:1–46. https://doi.org/10.1080/10643389.2020.1862551.

[69] Nawaz H, Zhang X, Chen S, You T, Xu F. Recent studies on cellulose-based fluorescent smart materials and their applications: A comprehensive review. Carbohydrate Polymers 2021:118135.

[70] Akter M, Bhattacharjee M, Dhar AK, Rahman FBA, Haque S, Rashid TU, et al. Cellulose-Based Hydrogels for Wastewater Treatment: A Concise Review. Gels 2021;7:30.

[71] Rana AK, Frollini E, Thakur VK. Cellulose nanocrystals: Pretreatments, preparation strategies, and surface functionalization. International Journal of Biological Macromolecules 2021;182:1554–81. https://doi.org/10.1016/j.ijbiomac.2021.05.119.

[72] Thakur VK, Voicu SI. Recent advances in cellulose and chitosan based membranes for water purification: a concise review. Carbohydrate Polymers 2016;146:148–65.

[73] Gianfreda L, Rao MA, Scelza R, de la Luz Mora M. Chapter 6 - Role of Enzymes in Environment Cleanup/Remediation. In: Dhillon GS, Kaur S, editors. Agro-Industrial Wastes as Feedstock for Enzyme Production, San Diego: Academic Press; 2016, p. 133–55. https://doi.org/10.1016/B978-0-12-802392-1.00006-X.

[74] Rana AK, Potluri P, Thakur VK. Cellulosic Grewia Optiva Fibres: Towards Chemistry, Surface Engineering and Sustainable Materials. Journal of Environmental Chemical Engineering 2021:106059. https://doi.org/10.1016/j.jece.2021.106059.

[75] Khandaker S, Chowdhury MF, Awual MR, Islam A, Kuba T. Efficient cesium encapsulation from contaminated water by cellulosic biomass based activated wood charcoal. Chemosphere 2021;262:127801.

[76] Hasan MM, Shenashen MA, Hasan MN, Znad H, Salman MS, Awual MR. Natural biodegradable polymeric bioadsorbents for efficient cationic dye encapsulation from wastewater. Journal of Molecular Liquids 2021;323:114587.

[77] Yeamin MB, Islam MM, Chowdhury A-N, Awual MR. Efficient encapsulation of toxic dyes from wastewater using several biodegradable natural polymers and their composites. Journal of Cleaner Production 2021;291:125920.

[78] Heinze T, Liebert T. Unconventional methods in cellulose functionalization. Progress in Polymer Science 2001;26:1689–762.

[79] Habibi Y, Lucia LA, Rojas OJ. Cellulose nanocrystals: chemistry, self-assembly, and applications. Chemical Reviews 2010;110:3479–500.

[80] Singh G, Singh G, Kang TS. Colloidal systems of surface active ionic liquids and sodium carboxymethyl cellulose: physicochemical investigations and preparation of magnetic nano-composites. Physical Chemistry Chemical Physics 2018;20:18528–38.

[81] Mubashir M, Dumée LF, Fong YY, Jusoh N, Lukose J, Chai WS, et al. Cellulose acetate-based membranes by interfacial engineering and integration of ZIF-62 glass nanoparticles for CO2 separation. Journal of Hazardous Materials 2021;415:125639.

[82] Ioelovich MY. Models of supramolecular structure and properties of cellulose. Polymer Science Series A 2016;58:925–43.

[83] Collazo-Bigliardi S, Ortega-Toro R, Chiralt Boix A. Isolation and characterisation of microcrystalline cellulose and cellulose nanocrystals from coffee husk and comparative study with rice husk. Carbohydrate Polymers 2018;191:205–15. https://doi.org/10.1016/j.carbpol.2018.03.022.

[84] Yim SM, Song JE, Kim HR. Production and characterization of bacterial cellulose fabrics by nitrogen sources of tea and carbon sources of sugar. Process Biochemistry 2017;59:26–36. https://doi.org/10.1016/j.procbio.2016.07.001.

[85] Schneider R, Hanak T, Persson S, Voigt CA. Cellulose and callose synthesis and organization in focus, what's new? Current Opinion in Plant Biology 2016;34:9–16.

[86] Geng H. A one-step approach to make cellulose-based hydrogels of various transparency and swelling degrees. Carbohydrate Polymers 2018;186:208–16. https://doi.org/10.1016/j.carbpol.2018.01.031.

[87] Hussain I, Sayed SM, Liu S, Oderinde O, Kang M, Yao F, et al. Enhancing the mechanical properties and self-healing efficiency of hydroxyethyl cellulose-based conductive hydrogels via supramolecular interactions. European Polymer Journal 2018;105:85–94. https://doi.org/10.1016/j.eurpolymj.2018.05.025.

[88] Isobe N, Komamiya T, Kimura S, Kim U-J, Wada M. Cellulose hydrogel with tunable shape and mechanical properties: From rigid cylinder to soft scaffold. International Journal of Biological Macromolecules 2018;117:625–31. https://doi.org/10.1016/j.ijbiomac.2018.05.071.

[89] Kanikireddy V, Varaprasad K, Jayaramudu T, Karthikeyan C, Sadiku R. Carboxymethyl cellulose-based materials for infection control and wound healing: A review. International Journal of Biological Macromolecules 2020.

[90] Javanbakht S, Shaabani A. Carboxymethyl cellulose-based oral delivery systems. International Journal of Biological Macromolecules 2019;133:21–9.

[91] Pettignano A, Charlot A, Fleury E. Carboxyl-functionalized derivatives of carboxymethyl cellulose: Towards advanced biomedical applications. Polymer Reviews 2019;59:510–60.

[92] Dutta SD, Patel DK, Lim K-T. Functional cellulose-based hydrogels as extracellular matrices for tissue engineering. Journal of Biological Engineering 2019;13:55.

[93] Chang C, Zhang L. Cellulose-based hydrogels: Present status and application prospects. Carbohydrate Polymers 2011;84:40–53.

[94] Seddiqi H, Oliaei E, Honarkar H, Jin J, Geonzon LC, Bacabac RG, et al. Cellulose and its derivatives: Towards biomedical applications. Cellulose 2021:1–39.

[95] Sjahro N, Yunus R, Abdullah LC, Rashid SA, Asis AJ, Akhlisah ZN. Recent advances in the application of cellulose derivatives for removal of contaminants from aquatic environments. Cellulose 2021:1–37.

[96] Bashari A, Rouhani Shirvan A, Shakeri M. Cellulose-based hydrogels for personal care products. Polymers for Advanced Technologies 2018;29:2853–67.

[97] An H, Bo Y, Chen D, Wang Y, Wang H, He Y, et al. Cellulose-based self-healing hydrogel through boronic ester bonds with excellent biocompatibility and conductivity. RSC Advances 2020;10:11300–10.

[98] Singha AS, Shama A, Thakur VK. X-Ray Diffraction, Morphological, and Thermal Studies on Methylmethacrylate Graft Copolymerized Saccharum ciliare Fiber. International Journal of Polymer Analysis and Characterization 2008;13:447–62. https://doi.org/10.1080/10236660802399747.

[99] Thakur VK, Singha AS, Misra BN. Graft copolymerization of methyl methacrylate onto cellulosic biofibers. Journal of Applied Polymer Science 2011;122:532–44. https://doi.org/10.1002/app.34094.

[100] Singha AS, Thakur VK. Fabrication of Hibiscus sabdariffa fibre reinforced polymer composites. Iran Polym J 2008;17:541–53.

[101] Thakur VK, Singha AS, Thakur MK. Fabrication and Physico-Chemical Properties of High-Performance Pine Needles/Green Polymer Composites. International Journal of Polymeric Materials and Polymeric Biomaterials 2013;62:226–30. https://doi.org/10.1080/00914037.2011.641694.

[102] Singha AS, Kumar Thakur V. Saccaharum Cilliare Fiber Reinforced Polymer Composites. E-Journal of Chemistry 2008;5:782–91. https://doi.org/10.1155/2008/941627.

[103] Singha AS, Thakur VK. Synthesis, Characterisation and Analysis of Hibiscus Sabdariffa Fibre Reinforced Polymer Matrix Based Composites. Polymers and Polymer Composites 2009;17:189–94. https://doi.org/10.1177/096739110901700308.

[104] Ashrafizadeh M, Ahmadi Z, Mohamadi N, Zarrabi A, Abasi S, Dehghannoudeh G, et al. Chitosan-based advanced materials for docetaxel and paclitaxel delivery: Recent advances and future directions in cancer theranostics. International Journal of Biological Macromolecules 2020;145:282–300. https://doi.org/10.1016/j.ijbiomac.2019.12.145.

[105] Shakeri S, Ashrafizadeh M, Zarrabi A, Roghanian R, Afshar EG, Pardakhty A, et al. Multifunctional Polymeric Nanoplatforms for Brain Diseases Diagnosis, Therapy and Theranostics. Biomedicines 2020;8:13. https://doi.org/10.3390/biomedicines8010013.

[106] Ashrafizadeh M, Mirzaei S, Gholami MH, Hashemi F, Zabolian A, Raei M, et al. Hyaluronic acid-based nanoplatforms for doxorubicin: A review of stimuli-responsive carriers, co-delivery and resistance suppression. Carbohydrate Polymers 2021:118491. https://doi.org/10.1016/j.carbpol.2021.118491.

[107] Tongdeesoontorn W, Mauer LJ, Wongruong S, Sriburi P, Rachtanapun P. Physical and Antioxidant Properties of Cassava Starch–Carboxymethyl Cellulose Incorporated with Quercetin and TBHQ as Active Food Packaging. Polymers 2020;12:366.

[108] Li D, Tian X, Wang Z, Guan Z, Li X, Qiao H, et al. Multifunctional adsorbent based on metal-organic framework modified bacterial cellulose/chitosan composite aerogel for high efficient removal of heavy metal ion and organic pollutant. Chemical Engineering Journal 2020;383:123127.

[109] Sharmila G, Muthukumaran C, Kirthika S, Keerthana S, Kumar NM, Jeyanthi J. Fabrication and characterization of Spinacae olareacea extract incorporated alginate/carboxymethyl cellulose microporous scaffold for bone tissue engineering. International Journal of Biological Macromolecules 2020.

[110] Garg KK, Prasad B. Treatment of toxic pollutants of purified terephthalic acid waste water: A review. Environmental Technology & Innovation 2017;8:191–217. https://doi.org/10.1016/j.eti.2017.07.001.

[111] Jiménez S, Micó MM, Arnaldos M, Medina F, Contreras S. State of the art of produced water treatment. Chemosphere 2018;192:186–208. https://doi.org/10.1016/j.chemosphere.2017.10.139.

[112] Awual MR. An efficient composite material for selective lead (II) monitoring and removal from wastewater. Journal of Environmental Chemical Engineering 2019;7:103087.

[113] Shi K, Ren M, Zhitomirsky I. Activated carbon-coated carbon nanotubes for energy storage in supercapacitors and capacitive water purification. ACS Sustainable Chemistry & Engineering 2014;2:1289–98.

[114] Di Natale F, Erto A, Lancia A. Desorption of arsenic from exhaust activated carbons used for water purification. Journal of Hazardous Materials 2013;260:451–8. https://doi.org/10.1016/j.jhazmat.2013.05.055.

[115] Huang T, Zhou R, Cui J, Zhang J, Tang X, Chen S, et al. Fast and cost-effective preparation of antimicrobial zinc oxide embedded in activated carbon composite for water purification applications. Materials Chemistry and Physics 2018;206:124–9. https://doi.org/10.1016/j.matchemphys.2017.11.044.

[116] Kosaka K, Iwatani A, Takeichi Y, Yoshikawa Y, Ohkubo K, Akiba M. Removal of haloacetamides and their precursors at water purification plants applying ozone/biological activated carbon treatment. Chemosphere 2018;198:68–74. https://doi.org/10.1016/j.chemosphere.2018.01.093.

[117] Lompe KM, Menard D, Barbeau B. Performance of biological magnetic powdered activated carbon for drinking water purification. Water Research 2016;96:42–51. https://doi.org/10.1016/j.watres.2016.03.040.

[118] Sarasidis VC, Plakas KV, Karabelas AJ. Novel water-purification hybrid processes involving in-situ regenerated activated carbon, membrane separation and advanced oxidation. Chemical Engineering Journal 2017;328:1153–63. https://doi.org/10.1016/j.cej.2017.07.084.

[119] Awual MR. A novel facial composite adsorbent for enhanced copper (II) detection and removal from wastewater. Chemical Engineering Journal 2015;266:368–75.

[120] Abdel Ghaffar AM, El-Arnaouty MB, Abdel Baky AA, Shama SA. Radiation Synthesis of Carboxymethyl Cellulose Hydrogels for Removal of Organic Contaminants from Its Aqueous Solution. Journal of Vinyl and Additive Technology 2019.

[121] Gupta V, Raja C, Anandkumar J. Phenol Removal by Novel Choline Chloride Blended Cellulose Acetate-Fly Ash Composite Membrane. Periodica Polytechnica Chemical Engineering 2020;64:116–23.

[122] Aouada FA, Pan Z, Orts WJ, Mattoso LH. Removal of paraquat pesticide from aqueous solutions using a novel adsorbent material based on polyacrylamide and methylcellulose hydrogels. Journal of Applied Polymer Science 2009;114:2139–48.

[123] Yu Z, Hu C, Dichiara AB, Jiang W, Gu J. Cellulose Nanofibril/Carbon Nanomaterial Hybrid Aerogels for Adsorption Removal of Cationic and Anionic Organic Dyes. Nanomaterials 2020;10:169.

[124] Chen X, Liu L, Luo Z, Shen J, Ni Q, Yao J. Facile preparation of a cellulose-based bioadsorbent modified by hPEI in heterogeneous system for high-efficiency removal of multiple types of dyes. Reactive and Functional Polymers 2018;125:77–83.

[125] Salama A. Preparation of CMC-gP (SPMA) super adsorbent hydrogels: Exploring their capacity for MB removal from waste water. International Journal of Biological Macromolecules 2018;106:940–6.

[126] Varaprasad K, Jayaramudu T, Sadiku ER. Removal of dye by carboxymethyl cellulose, acrylamide and graphene oxide via a free radical polymerization process. Carbohydrate Polymers 2017;164:186–94.

[127] Song X, Chen F, Liu S. A Lignin-containing Hemicellulose-based Hydrogel and its Adsorption Behavior. BioResources 2016;11:6378–92.

[128] Dai H, Huang H. Modified pineapple peel cellulose hydrogels embedded with sepia ink for effective removal of methylene blue. Carbohydrate Polymers 2016;148:1–10.

[129] Mohammed N, Grishkewich N, Berry RM, Tam KC. Cellulose nanocrystal–alginate hydrogel beads as novel adsorbents for organic dyes in aqueous solutions. Cellulose 2015;22:3725–38.

[130] El-Kelesh NA, Mahmoud GA. Synthesis and properties of treated waste cellulose and GMA grafted composite to remove different acid dyes from aqueous solutions. Cellul Chem Technol 2015;49:881–9.

[131] Saber-Samandari S, Saber-Samandari S, Heydaripour S, Abdouss M. Novel carboxymethyl cellulose based nanocomposite membrane: Synthesis, characterization and application in water treatment. Journal of Environmental Management 2016;166:457–65.

[132] Zulfiqar S, Rafique U, Akhtar MJ. Removal of pirimicarb from agricultural waste water using cellulose acetate–modified ionic liquid membrane. Environmental Science and Pollution Research 2019;26:15795–802.

[133] Liang X, Liang B, Wei J, Zhong S, Zhang R, Yin Y, et al. A cellulose-based adsorbent with pendant groups of quaternary ammonium and amino for enhanced capture of aqueous Cr (VI). International Journal of Biological Macromolecules 2020.

[134] Liu S, Cheng G, Xiong Y, Ding Y, Luo X. Adsorption of low concentrations of bromide ions from water by cellulose-based beads modified with TEMPO-mediated oxidation and Fe (III) complexation. Journal of Hazardous Materials 2020;384:121195.

[135] Wu Q, He H, Zhou H, Xue F, Zhu H, Zhou S, et al. Multiple active sites cellulose-based adsorbent for the removal of low-level Cu (II), Pb (II) and Cr (VI) via multiple cooperative mechanisms. Carbohydrate Polymers 2020:115860.

[136] Li S-S, Wang X-L, An Q-D, Xiao Z-Y, Zhai S-R, Cui L, et al. Upon designing carboxyl methylcellulose and chitosan-derived nanostructured sorbents for efficient removal of Cd (II) and Cr (VI) from water. International Journal of Biological Macromolecules 2020;143:640–50.

[137] Ding J, Li Q, Xu X, Zhang X, Su Y, Yue Q, et al. A wheat straw cellulose-based hydrogel for Cu (II) removal and preparation copper nanocomposite for reductive degradation of chloramphenicol. Carbohydrate Polymers 2018;190:12–22.

[138] Li Y, Chen MD, Wan X, Zhang L, Wang X, Xiao H. Solvent-free synthesis of the cellulose-based hybrid beads for adsorption of lead ions in aqueous solutions. RSC Advances 2017;7:53899–906.

[139] Wang F, Pan Y, Cai P, Guo T, Xiao H. Single and binary adsorption of heavy metal ions from aqueous solutions using sugarcane cellulose-based adsorbent. Bioresource Technology 2017;241:482–90.

[140] Ge H, Huang H, Xu M, Chen Q. Cellulose/poly (ethylene imine) composites as efficient and reusable adsorbents for heavy metal ions. Cellulose 2016;23:2527–37.

[141] Wang J, Wei L, Ma Y, Li K, Li M, Yu Y, et al. Collagen/cellulose hydrogel beads reconstituted from ionic liquid solution for Cu (II) adsorption. Carbohydrate Polymers 2013;98:736–43.

[142] Saber-Samandari S, Saber-Samandari S, Gazi M. Cellulose-graft-polyacrylamide/hydroxyapatite composite hydrogel with possible application in removal of Cu (II) ions. Reactive and Functional Polymers 2013;73:1523–30.

[143] Ahmed A-S, El-Masry AM, Saleh A, Nada A. Bagasse hydrogels: water absorption and ions uptake. Pigment & Resin Technology 2013;42:68–78.

[144] Zhao L, Mitomo H. Adsorption of heavy metal ions from aqueous solution onto chitosan entrapped CM-cellulose hydrogels synthesized by irradiation. Journal of Applied Polymer Science 2008;110:1388–95.

[145] Mittal H, Al Alili A, Morajkar PP, Alhassan SM. GO crosslinked hydrogel nanocomposites of chitosan/carboxymethyl cellulose–A versatile adsorbent for the treatment of dyes contaminated wastewater. International Journal of Biological Macromolecules 2021;167:1248–61.

[146] Chen X, Liu L, Luo Z, Shen J, Ni Q, Yao J. Facile preparation of a cellulose-based bioadsorbent modified by hPEI in heterogeneous system for high-efficiency removal of multiple types of dyes. Reactive and Functional Polymers 2018;125:77–83.

[147] Chen M-L, Chen M-L, Chen X-W, Wang J-H. Functionalization of MWNTs with hyperbranched PEI for highly selective isolation of BSA. Macromolecular Bioscience 2010;10:906–15.

[148] Maneerung T, Liew J, Dai Y, Kawi S, Chong C, Wang C-H. Activated carbon derived from carbon residue from biomass gasification and its application for dye adsorption: kinetics, isotherms and thermodynamic studies. Bioresource Technology 2016;200:350–9.

[149] Fundador NGV, Enomoto-Rogers Y, Takemura A, Iwata T. Syntheses and characterization of xylan esters. Polymer 2012;53:3885–93.

[150] Hamcerencu M, Desbrieres J, Khoukh A, Popa M, Riess G. Synthesis and characterization of new unsaturated esters of Gellan Gum. Carbohydrate Polymers 2008;71:92–100.

[151] Yan C, Zhang J, Jiasong H, Huiquan LI, Zhang Y. Homogeneous acetylation of cellulose at relatively high concentrations in an ionic liquid. Chinese Journal of Chemical Engineering 2010;18:515–22.

[152] Zhang YD, Xia XZ. Physicochemical Characteristics of pineapple (Ananas mill.) peel cellulose prepared by different methods. Advanced Materials Research, vol. 554, Trans Tech Publ; 2012, p. 1038–41.

[153] Lezehari M, Basly J-P, Baudu M, Bouras O. Alginate encapsulated pillared clays: removal of a neutral/anionic biocide (pentachlorophenol) and a cationic dye (safranine) from aqueous solutions. Colloids and Surfaces A: Physicochemical and Engineering Aspects 2010;366:88–94.

[154] Liu L, Wan Y, Xie Y, Zhai R, Zhang B, Liu J. The removal of dye from aqueous solution using alginate-halloysite nanotube beads. Chemical Engineering Journal 2012;187:210–6.

[155] Godiya CB, Cheng X, Li D, Chen Z, Lu X. Carboxymethyl cellulose/polyacrylamide composite hydrogel for cascaded treatment/reuse of heavy metal ions in wastewater. Journal of Hazardous Materials 2019;364:28–38.

[156] Singh N, Kumari S, Goyal N, Khan S. Al2O3/GO cellulose based 3D-hydrogel for efficient fluoride removal from water. Environmental Nanotechnology, Monitoring & Management 2021;15:100444.

[157] Ciolacu D, Oprea AM, Anghel N, Cazacu G, Cazacu M. New cellulose–lignin hydrogels and their application in controlled release of polyphenols. Materials Science and Engineering: C 2012;32:452–63.

[158] Singh B, Chauhan GS, Kumar S, Chauhan N. Synthesis, characterization and swelling responses of pH sensitive psyllium and polyacrylamide based hydrogels for the use in drug delivery (I). Carbohydrate Polymers 2007;67:190–200.

[159] Zhang D, Wang L, Zeng H, Yan P, Nie J, Sharma VK, et al. A three-dimensional macroporous network structured chitosan/cellulose biocomposite sponge for rapid and selective removal of mercury (II) ions from aqueous solution. Chemical Engineering Journal 2019;363:192–202.

[160] Nascimento DM, Nunes YL, Figueirêdo MC, de Azeredo HM, Aouada FA, Feitosa JP, et al. Nanocellulose nanocomposite hydrogels: technological and environmental issues. Green Chemistry 2018;20:2428–48.

[161] Ma J, Li X, Bao Y. Advances in cellulose-based superabsorbent hydrogels. RSC Advances 2015;5:59745–57.

[162] Asadi N, Pazoki-Toroudi H, Del Bakhshayesh AR, Akbarzadeh A, Davaran S, Annabi N. Multifunctional hydrogels for wound healing: Special focus on biomacromolecular based hydrogels. International Journal of Biological Macromolecules 2020.

[163] Zhang J, Wu J, Yu J, Zhang X, He J, Zhang J. Application of ionic liquids for dissolving cellulose and fabricating cellulose-based materials: state of the art and future trends. Materials Chemistry Frontiers 2017;1:1273–90.

[164] Tan J, Xie S, Wang G, Yu CW, Zeng T, Cai P, et al. Fabrication and optimization of the thermo-sensitive hydrogel carboxymethyl cellulose/poly (N-isopropylacrylamide-co-acrylic acid) for U (VI) removal from aqueous solution. Polymers 2020;12:151.

[165] Feng H, Li J, Wang L. Preparation of biodegradable flax shive cellulose-based superabsorbent polymer under microwave irradiation. BioResources 2010;5:1484–95.

[166] Zhang M, Wan Y, Wen Y, Li C, Kanwal A. A novel Poly (vinyl alcohol)/carboxymethyl cellulose/yeast double degradable hydrogel with yeast foaming and double degradable property. Ecotoxicology and Environmental Safety 2020;187:109765.

[167] Munjur HM, Hasan MN, Awual MR, Islam MM, Shenashen MA, Iqbal J. Biodegradable natural carbohydrate polymeric sustainable adsorbents for efficient toxic dye removal from wastewater. Journal of Molecular Liquids 2020;319:114356.

[168] Chandel N, Sharma K, Sudhaik A, Raizada P, Hosseini-Bandegharaei A, Thakur VK, et al. Magnetically separable ZnO/ZnFe2O4 and ZnO/CoFe2O4 photocatalysts supported onto nitrogen doped graphene for photocatalytic degradation of toxic dyes. Arabian Journal of Chemistry 2020;13:4324–40. https://doi.org/10.1016/j.arabjc.2019.08.005.

[169] Raizada P, Thakur P, Sudhaik A, Singh P, Thakur VK, Hosseini-Bandegharaei A. Fabrication of dual Z-scheme photocatalyst via coupling of BiOBr/Ag/AgCl heterojunction with P and S co-doped g-C3N4 for efficient phenol degradation. Arabian Journal of Chemistry 2020;13:4538–52. https://doi.org/10.1016/j.arabjc.2019.10.001.

[170] Hasija V, Raizada P, Sudhaik A, Singh P, Thakur VK, Khan AAP. Fabrication of Ag/AgI/WO3 heterojunction anchored P and S co-doped graphitic carbon nitride as a dual Z scheme photocatalyst for efficient dye degradation. Solid State Sciences 2020;100:106095. https://doi.org/10.1016/j.solidstatesciences.2019.106095.

[171] Kumar A, Raizada P, Hosseini-Bandegharaei A, Kumar Thakur V, Nguyen V-H, Singh P. C-, N-Vacancy defect engineered polymeric carbon nitride towards photocatalysis: viewpoints and challenges. Journal of Materials Chemistry A 2021;9:111–53. https://doi.org/10.1039/D0TA08384D.

[172] Ahmad N, Anae J, Khan MZ, Sabir S, Yang XJ, Thakur VK, et al. Visible light-conducting polymer nanocomposites as efficient photocatalysts for the treatment of organic pollutants in wastewater. Journal of Environmental Management 2021;295:113362. https://doi.org/10.1016/j.jenvman.2021.113362.

[173] Jiang Y, Lawan I, Zhou W, Zhang M, Fernando GF, Wang L, et al. Synthesis, properties and photocatalytic activity of a semiconductor/cellulose composite for dye degradation-a review. Cellulose 2020;27:595–609.

[174] Kumar R, Raizada P, Verma N, Hosseini-Bandegharaei A, Thakur VK, Le QV, et al. Recent advances on water disinfection using bismuth based modified photocatalysts: Strategies and challenges. Journal of Cleaner Production 2021;297:126617. https://doi.org/10.1016/j.jclepro.2021.126617.

[175] Chen Y, Xiang Z, Wang D, Kang J, Qi H. Effective photocatalytic degradation and physical adsorption of methylene blue using cellulose/GO/TiO 2 hydrogels. RSC Advances 2020;10:23936–43.

[176] Wang J, Li X, Cheng Q, Lv F, Chang C, Zhang L. Construction of β-FeOOH@ tunicate cellulose nanocomposite hydrogels and their highly efficient photocatalytic properties. Carbohydrate Polymers 2020;229:115470.

[177] Heidarpour H, Golizadeh M, Padervand M, Karimi A, Vossoughi M, Tavakoli MH. In-situ formation and entrapment of Ag/AgCl photocatalyst inside cross-linked carboxymethyl cellulose beads: A novel photoactive hydrogel for visible-light-induced photocatalysis. Journal of Photochemistry and Photobiology A: Chemistry 2020;398:112559.

[178] Tamaddon F, Mosslemin MH, Asadipour A, Gharaghani MA, Nasiri A. Microwave-assisted preparation of ZnFe2O4@ methyl cellulose as a new nano-biomagnetic photocatalyst for photodegradation of metronidazole. International Journal of Biological Macromolecules 2020;154:1036–49.

[179] Beluns S, Gaidukovs S, Platnieks O, Gaidukova G, Mierina I, Grase L, et al. From Wood and Hemp Biomass Wastes to Sustainable Nanocellulose Foams. Industrial Crops and Products 2021; 170:113780. https://doi.org/10.1016/j.indcrop.2021.113780.

[180] Singha AS, Thakur VK. Grewia optiva Fiber Reinforced Novel, Low Cost Polymer Composites. E-Journal of Chemistry 2009; 6:71–6. https://doi.org/10.1155/2009/642946.

[181] Platnieks O, Sereda A, Gaidukovs S, Thakur VK, Barkane A, Gaidukova G, et al. Adding value to poly (butylene succinate) and nanofibrillated cellulose-based sustainable nanocomposites by applying masterbatch process. Industrial Crops and Products 2021; 169:113669. https://doi.org/10.1016/j.indcrop.2021.113669.